Science of Remote Sensing 13 (2026) 100374

Contents lists available at ScienceDirect

Science of Remote Sensing

journal homepage: www.sciencedirect.com/journal/science-of-remote-sensing

Utilising mobile laser scanning point clouds to assess harvesting quality in thinning stands

Anwar Sagar [a,b,*], Johannes Pohjala [c,**], Jesse Muhojoki [d], Anubhav Dhital [c], Harri Kaartinen [d], Kalle Kärhä [c], Kalervo Järvelin [e], Reza Ghabcheloo [b], Juha Hyyppä [d], Ville Kankare [f]

[a] Ponsse Plc, Korkeakoulunkatu 7, 33720, Tampere, Finland
[b] Faculty of Engineering and Natural Sciences, Tampere University, 33720, Tampere, Finland
[c] School of Forest Sciences, Faculty of Science, Forestry and Technology, University of Eastern Finland, Joensuu, Finland
[d] Department of Remote Sensing and Photogrammetry, Finnish Geospatial Research Institute (FGI), Espoo, Finland
[e] Faculty of Information Technology and Information Sciences, Tampere University, 33720, Tampere, Finland
[f] Department of Geography and Geology, Faculty of Science, University of Turku, Turku, Finland

ARTICLE INFO

Keywords:
Mobile laser scanning (MLS)
Forest management
Thinning
Advanced driver assistance systems (ADAS)
Stem defect
Harvesting quality

ABSTRACT

Forestry is entering a new era where precision and innovation converge through advanced mobile laser scanning (MLS) technologies. Traditional methods of assessing harvesting quality, often manual, time-consuming, and prone to human error, are being replaced by objective, data-driven approaches. In this study, we conducted high-resolution point cloud scanning across four forest stands (11 ha) in Central Finland using the handheld GeoSLAM ZEB Horizon LiDAR system. We aimed to evaluate the capacity of MLS to measure harvesting attributes related to stand density, tree dimensions, and strip road characteristics, to assess the impact of the Ponsse Plc Thinning Density Assistant (TDA), and to detect defective tree stems. Within a 5-ha subset, 11 potentially anomalous trees were identified. A spatially precise tree map was created using QGIS and a separate map application, enabling comparison between manual field measurements and digital measurements. The findings indicate a strong concordance between automated and traditional assessments. With few exceptions, the results were consistent with established Best Practices for Sustainable Forest Management. Preliminary tests of a novel algorithm for curved stem detection further suggest the potential of MLS for automated defect recognition. A strip road width model was also developed to estimate the average strip road width within the forest stand. These findings underscore MLS as a powerful tool for enhancing accuracy, efficiency, and objectivity in modern forest management.

Key finding:

- Defect identification is accurate, but tree detection deteriorates at low densities.
- Missed detections are caused by crown occlusion or suboptimal parameter settings.
- Lower point density reduces detected trees but not defect classification accuracy.
- Point clouds and derived tree maps reliably assess thinning quality.
- Thinning quality meets Finnish best-practice forest management guidelines.

1. Introduction

Forest thinning is one of the key silvicultural practices aimed at improving the growing conditions of residual trees, thereby enhancing the vitality, quality, and yield accumulation of the forest (Cameron, 2002; Zhang et al., 2024). Thinning can be carried out using various strategies, such as below-, above-, quality-, or systematic thinning,

* Corresponding author. Ponsse Plc, Korkeakoulunkatu 7, 33720, Tampere, Finland.
** Corresponding author.
E-mail address: anwar.sagar@tuni.fi (A. Sagar).

https://doi.org/10.1016/j.srs.2026.100374
Received 1 October 2025; Received in revised form 27 December 2025; Accepted 14 January 2026
Available online 16 January 2026

where the main difference lies in the selection of trees to be harvested (Niemistö et al., 2018; Kellomäki, 2022). However, all these strategies share a common goal of optimising competition dynamics and forest structure, removing damaged trees, and maintaining a balanced spatial distribution (Niemistö et al., 2018; Saarinen et al., 2020; Kellomäki, 2022; Kärhä et al., 2021). Consequently, forest management is recognised to have a significant impact on forest development by influencing the natural growth dynamics (Kellomäki, 2022). Even when meticulously planned, forest thinning can still adversely affect the forest by causing damage to soils, residual trees, water bodies, and habitats (Sirén, 1998; Ampoorter et al., 2012; Cambi et al., 2015).

The concept of harvesting quality includes several important attributes, such as thinning intensity, damage to trees and roots, tree selection, strip road width, spacing, and ruts (Sirén, 1998; Iittiläinen et al., 2003; Leivo et al., 2023). Initially, mechanised forest thinning raised concerns about the potential for greater damage to residual trees compared to motor-manual logging (Isomäki and Kallio, 1974; Lilleberg, 1984, 1986; Bettinger and Kellogg, 1993). Over time, advances in machinery, operator skills, and worksite planning have led to a decline in harvesting damage rates (Harstela, 1996). The 1980s and 1990s saw a peak in Scandinavian harvesting quality research, during which numerous methods were developed to evaluate key attributes such as residual tree damage (Siren, 1981, 1982), strip road width and spacing (Sondell, 1974; Arvidsson and Knutell, 1977; Bucht, 1977; Carlestål and Dehlén, 1977; Tørå, 1978; Diggle and Knutell, 1979; Björheden and Fröding, 1986; Isomäki and Niemistö, 1990; Isomäki, 1994), rutting (Ahlgren, 1982), and stand structure after thinning (Niemistö, 1992). Many of these methods remain widely used in Fennoscandia (Iittiläinen et al., 2003; Bergkvist and Staland, 2003; Leivo et al., 2023), as well as in other parts of the world (Strubergs et al., 2024; Laajalehto, 2025).

In Finland, the quality of harvesting is typically evaluated through field surveys conducted during or, more commonly, months after the thinning process. Assessing harvesting quality is time-consuming and expensive, resulting in limited data coverage relative to the number of forest thinnings (Sirén, 1998). To address this challenge, more automated methods have been developed (Ovaskainen, 2019). For instance, stand-specific attributes related to the strip road network—such as width and spacing—can be precisely determined using forest machines' Global Navigation Satellite System (GNSS) positioning, which is available in the harvesting production report (hpr) file via StanForD 2010; Arlinger et al., 2021; Hannrup et al. (2021); Ovaskainen and Riekki (2022); Strubergs et al. (2024). However, canopy-induced signal loss frequently hampers GNSS accuracy, restricting the ability to attain sub-metre positioning precision (Noordermeer et al., 2021; Faitli et al., 2024; Liu et al., 2025). Additionally, integrating remote sensing data with harvesting machines allows for more precise and real-time monitoring of forest conditions (Kankare et al., 2019; Korhonen et al., 2024).

Laser scanning technologies produce high-resolution three-dimensional (3D) point cloud data for capturing forest structure at different spatial resolutions (i.e., point density p/m2) (Liang et al., 2022). These technologies are used on three main platforms: 1) Airborne Laser Scanning (ALS) enables assessments from landscape to tree scale over large areas (Holmgren and Persson, 2004; White et al., 2013; Vastaranta et al., 2014; Yrttimaa et al., 2025); 2) Terrestrial Laser Scanning (TLS) records detailed, fine-scale information from static ground positions (Liang et al., 2016; Krishna Moorthy et al., 2020; Calders et al., 2020); and 3) Mobile Laser Scanning (MLS) collects dense, ground-level point cloud data dynamically from moving platforms (Di Stefano et al., 2021; Sevgen and Abdikan, 2023). Among these, MLS has become an emerging tool for real-time harvesting quality assessment, due to its ability to quickly acquire high-resolution 3D data while navigating complex environments (Bauwens et al., 2016; Salmivaara et al., 2018). Mounted on ground vehicles or forestry machinery, MLS systems combine Light Detection and Ranging (LiDAR) sensors with GNSS and Inertial Navigation System (INS), enabling accurate georeferencing of point clouds even under forest canopy conditions where airborne signals often weaken (Gollob et al., 2020). In forest structure evaluation, MLS has been used to characterise individual tree attributes such as stem diameter, height, volume, and biomass (Bauwens et al., 2016; Hyyppä et al., 2020a,b; Neudam et al., 2022; Faitli et al., 2024) and biodiversity indicators (Kafle et al., 2025). Liang et al. (2014) demonstrated that MLS offers a practical balance between accuracy and operational flexibility for forest monitoring. However, there remains a lack of point cloud processing methods (even in post-processing) to derive key harvesting quality features in real time from high-density point cloud data during forest operations. These methods aim to monitor harvesting quality throughout logging continuously, support the harvester operator, and provide real-time reports on harvesting quality.

Currently, forestry operations are increasingly adopting advanced technologies to address long-standing challenges in assessing harvest quality. Traditional methods rely heavily on field-based plot sampling, which, although informative, is inherently limited by spatial bias and logistical constraints. These limitations often cause assessments to overlook the true variability of harvesting impacts across diverse and heterogeneous forest landscapes. In contrast, laser scanning systems offer a transformative alternative, providing comprehensive, wall-to-wall spatial coverage that can eliminate uncertainties related to plot placement and density. For example, Xiang et al. (2024) introduced ForAINet, a deep learning framework capable of segmenting high-density ALS point clouds into individual trees and components across various forest types, achieving over 85 % F-score for individual tree segmentation. This approach enables detailed forest inventories, reducing the constraints of traditional sampling methods. When integrated into harvesting machinery, MLS technology also offers real-time feedback, allowing immediate assessment of operational parameters such as stump height, stem damage, soil disturbance, and residual stand condition. A study by Faitli et al. (2024) demonstrated the integration of an MLS system with a forest harvester, enabling accurate localisation and tree stem measurements both in real-time and through post-processing of collected point clouds. The system achieved a root-mean-square error of 3–4 cm in estimating diameter at breast height (DBH) in real-time mode and 2–3 cm depending on the distance of the trajectory, showcasing its effectiveness in delivering timely feedback during harvesting operations for future applications. This immediacy supports on-site adjustments by operators, preventing a decline in thinning quality.

Beyond feedback, laser scanning systems enhance decision-making by providing situational awareness tools that help navigate obstacles, optimise travel routes to minimise soil compaction, and identify sensitive areas that require careful handling. Crucially, the data collected are objective and standardised, reducing human error and enabling consistent comparisons across operators, sites, and time periods. Despite these advantages, significant challenges remain. The development of sensor-agnostic deep learning models, such as SegmentAnyTree, has further improved tree segmentation across various laser scanning platforms, supporting decision-making during complex forest operations (Wielgosz et al., 2024). Current laser scanning-based assessments often depend on post-processing techniques that are computationally intensive and require manual interpretation, limiting their real-time use. There is a pressing need to develop automated, efficient point cloud processing algorithms capable of extracting relevant harvesting quality metrics in operational environments. For instance, Ponsse Plc has introduced a system called the Thinning Density Assistance (TDA) system, which delivers real-time information on tree density and stand structure (Ponsse Plc.). Overcoming this technological gap is crucial to unlocking the full potential of laser scanning in forest management, transforming it from a reactive diagnostic tool to a proactive, real-time element of precision forestry.

Therefore, the primary objective of this research is to assess the consistency of MLS point cloud data in determining harvesting quality characteristics compared to conventional harvesting quality assessment methods. Specifically, we seek to examine the following research

questions (RQs):

RQ1: What is the capability of point cloud data in detecting defects in individual trees?
RQ2: To what extent can point cloud data, particularly from MLS, provide consistent and reliable measurements of harvesting quality attributes such as strip road spacing during first and later thinning operations, in comparison to conventional assessment methods?
RQ3: Does the use of TDA as a treatment influence harvesting quality outcomes, and if so, in what ways?

A schematic representation of the study process is shown in Fig. 1.

2. Materials and methods

2.1. Experimental design and study area

The study area is located in northern Central Finland, specifically within the Saarijärvi-Viitasaari and Kuopio regions, where the landscape is shaped by boreal forest ecosystems (Table 1 and Fig. 2). Finland is located in northern Europe, extending between latitudes 60° and 70° N and longitudes 20° and 32° E. The 3 experimental forest sites, encompassing four stands and 10.5 ha, were harvested in 2023 (Pohjala et al., 2025). To facilitate systematic analysis, forest stands were subdivided into 44 sample plots, intended to be evenly distributed. However, variations in plot size and spacing occurred due to forest conditions, technical limitations, and operational interruptions. The experimental sites were dominated by Scots pine (*Pinus sylvestris* L.) or Silver Birch (*Betula pendula*) trees, a keystone species in Finland's boreal biome, interspersed

Table 1
Details and geographical coordinates of the study stands where the experiment was carried out. DBH at (1.3 m) reference (Pohjala et al., 2025).

Stand number		1	2	3	4
Location		Kyyjärvi	Karstula	Kuopio	Kuopio
Northing	WGS 84	63°02′05.9″	62°49′56.4″	62°53′02.2″	62°53′13.6″
Easting	WGS 84	24°42′56.3″	24°30′19.2″	27°11′51.0″	27°11′31.4″
Soil type		Peatland	Mineral soil	Mineral soil	Mineral soil
Forest type		Sub-xeric peat heath	Sub-Xeric Heath	Herb-rich Heath	Herb-rich Heath
Treatment		First thinning	Later thinning	First thinning	Later thinning
Preclearing		No	No	Yes	No
Stand age	Years	37	55	27	42
Main species		*Pinus sylvestris*	*Pinus sylvestris*	*Betula pendula*	*Betula pendula*
Mean DBH	cm	15.6	18.0	13.8	16.1
Mean height	m	15.1	17.5	17.8	17.8
Dominant height	m	17.0	20.4	18.0	20.4
Number of trees	trees ha^{-1}	1137	896	1277	875
Initial stocking	m^3 ha^{-1}	198	262	138	193
Stand area	ha	2.6	4.3	1.6	1.9

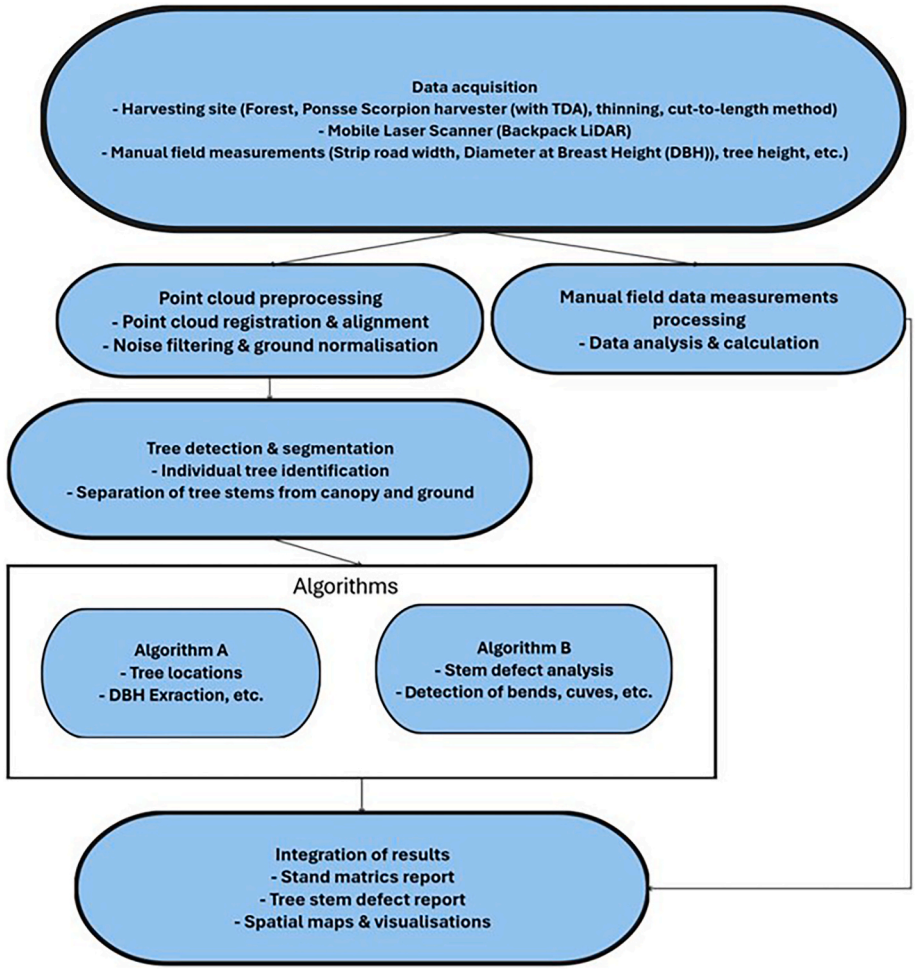

Fig. 1. Overview of the data acquisition, preprocessing, algorithmic analysis, and result integration steps used in this study.

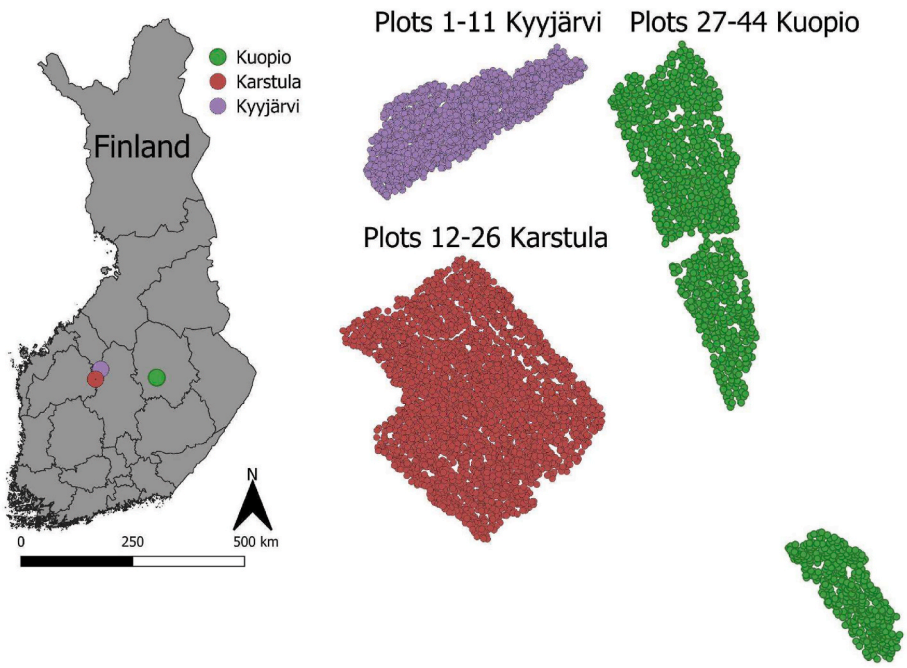

Fig. 2. Location of the test area and forest stand. Geographical map of Finland showing the locations of the three study sites: Kyyjärvi, Karstula, and Kuopio. The experimental plots are numbered as follows: 1–11 in Kyyjärvi, 12–26 in Karstula, and 27–44 in Kuopio.

with occasional ash (*Fraxinus excelsior*) and Norway spruce (*Picea abies* (L.) Karst.). Fig. 2 presents a geographical map of Finland indicating the locations of the three study sites. Forest type was determined according to (Cajander, 1926).

At the experimental sites, a cut-to-length (CTL) harvester, specifically the Ponsse Scorpion harvester (Ponsse Plc), was used to conduct thinning operations. The CTL method, developed to address traditional cutting operations' inefficiencies and environmental concerns, involves felling, delimbing, and bucking trees directly at the harvesting site. The thinning was carried out as low thinning, where the machine operators selected poor-quality and suppressed trees for removal. The forest machine operators who participated in this study were skilled, and their productivity was at the average level in the Scandinavian region, approximately 18 m^3 per effective machine hour (E_0^{-1}) (Pohjala et al., 2025).

The Ponsse Scorpion harvester (21,000–22,500 kg) features an 11 m crane reach, an 8-wheel chassis with active suspension for stability, and a centrally mounted C50+ crane with a rotating cabin for full operator visibility. Crane and head functions were managed through the OptiControl system, while the Opti 5G system combined GNSS and LiDAR measurements to support stand mapping and integration with the TDA system for real-time information on tree density and structure. Threshold outputs guided selective thinning and generated data for monitoring and evaluation. Processed timber was forwarded by a Ponsse Buffalo forwarder (14–15 t load capacity, 17,500–19,500 kg, optional 10 m crane reach), with OptiControl supporting efficient loading and transport under variable terrain conditions (Ponsse Plc, 2022).

2.2. Data acquisition

2.2.1. Field survey

The field survey served as a reference in this study. The harvesting quality assessment included dominant tree height (m), arithmetic mean diameter at breast height (DBH, cm), tree density (trees ha^{-1}), basal area (m^2 ha^{-1}), strip road width (m), distance between strip roads (m), and thinning intensity, expressed as the percentage of trees removed relative to those left standing (%). In addition, we conducted a complete survey of the stand to record harvesting damage, expressed as the proportion (%) of residual trees that showed visible injuries such as stem wounds or bark removal, using conventional field assessment methods (Leivo et al., 2023).

Several measurement tools were employed to gather precise forest characteristics, including a meter (Hultafors AB talmeter), a logger's tape (Spencer 20 m), a hypsometer, and a relascope (an angle gauge). Each instrument served a specific purpose in capturing critical data to inform the analysis. The meter was utilised for measuring tree DBH, a logger's tape to measure distances from the centre of each plot, and the measurement distance required for assessing tree height. Additionally, it was employed to measure the strip road width and the spacing between two parallel strip roads, ensuring accurate spatial mapping of the machinery's operational footprint.

The hypsometer (Suunto PM5-1520 PC) was specifically used to determine tree height with an accuracy of ±2 % (Suunto, 2025). This precision instrument facilitated accurate height measurements by allowing the operator to calculate vertical dimensions relative to the measured distance and angles recorded. Finally, the relascope was employed to estimate the basal area per hectare. This was achieved by measuring the apparent angular width of a tree from the observer's perspective, enabling a rapid and efficient assessment of stand density. Together, these tools provided a comprehensive dataset for evaluating the structural and spatial characteristics of the study forest.

During the field survey, a standardised protocol was employed to ensure consistency across all the established 44 sample plots. The field survey method was based on the guidelines of Iittiläinen et al. (2003), applied to single strip road plots. Each plot was subjected to three measurement points, with the spatial distribution of these points contingent upon the total length of the plot. For plots measuring 100 m (m) or less, the first measurement was conducted 10 m from the starting boundary, followed by subsequent measurements at 20-m intervals. In contrast, for plots exceeding 100 m in length, measurements were initiated at 20 m from the plot origin, with the following two points spaced at 40-m intervals.

At each designated measurement location, data collection commenced from the central axis of the harvester trail. From this centreline, a lateral extension of 2.82 m was measured to both the right and left, delineating a circular sampling area of 100 m^2 with a radius of 5.64

m. All trees falling within this radius were identified and categorised according to tree species type. For each tree species type observed within the sampling circle, two specific trees were selected for further measurement: the second largest and the second smallest, based on diameter. According to Niemistö (1992), this is the most unbiased estimate of the arithmetic mean DBH, if not all trees on the circle plot are counted. The weighted average DBH is calculated based on the relative proportions of different tree species. The weighted DBH is given by

$$\text{Weighted } DBH = \frac{\sum_{i=1}^{n} (density_i \times DBH_i)}{\sum_{i=1}^{n} density_i}, \quad (1)$$

where $density_i$ denotes the number of trees per ha for species i, DBH_i the average diameter at breast height for species i and n the total number of species. This formulation ensures that species with a higher number of trees exert a greater influence on the overall average DBH.

All trees with a DBH exceeding 7 cm were measured in the sample plots if they were at least half of the dominant height. Dominant height was estimated by measuring the height of the tallest tree by DBH in the circular plot (Niemistö, 1992). Dominant height (also referred to as top height), as used in this study, refers to the average height of the 100 largest-diameter trees per hectare in the stand, as defined according to IUFRO standards (Tarmu et al., 2020).

Along with individual tree measurements, the total number of trees within the circular plot was recorded to assess stand density. The basal area was calculated using a relascope, a device designed for quick optical measurement of cross-sectional tree area at breast height. Additionally, the outer width of the strip road and the spacing between strip roads (i.e., the distance between adjacent strip roads) were measured to gain a comprehensive understanding of stand structure and machinery influence. This systematic approach ensured the collection of reliable, spatially representative data across different plot lengths and forest conditions.

The initial stand conditions were determined using the harvester production (hpr) file, which included plot-wise information for every processed stem (species, DBH, volume, assortments, etc.) as well as densities and DBH data from the remaining trees from MLS. The number of removed trees and the basal area were calculated by dividing these values by the plot area.

2.2.2. Mobile laser scanning

The experimental MLS setup consisted of a backpack-mounted system equipped with a suite of advanced technologies, including a ZEB Horizon sensor head with laser scanner, IMU, and 360 camera from GeoSLAM Ltd. (GeoSLAM, 2025) (Fig. 3). Zeb Horizon features a laser range of up to 100 m, a 360° × 270° field of view, ranging accuracy of 1–3 cm (1σ), and a point measurement speed of up to 300,000 points per second. It uses GeoSLAM's proprietary SLAM (Simultaneous Localisation and Mapping) algorithm. To conduct the survey, the system was carried by the researcher as they walked through the forest stand. Following the harvester strip roads that reflected the topography of the site, the researcher systematically scanned the forest to ensure comprehensive coverage of the study area. This method facilitated the collection of high-resolution spatial and structural point cloud data across the entire site, providing a detailed representation of the forest's characteristics, capable of locating trees with less than 15 cm precision (Muhojoki et al., 2024).

Individual plots were scanned separately using MLS equipment. To ensure the integrity and manageability of the SLAM (Simultaneous Localisation and Mapping) processing, data collection with the ZEB Horizon system was strategically segmented. Instead of capturing the entire test site in a single acquisition, the survey was divided into multiple sections aligned with the harvester strip roads that naturally partitioned the area. Each section was scanned individually to prevent the creation of large datasets, which could compromise processing efficiency and accuracy. To minimise cumulative drift — a known challenge in SLAM-based systems — the data acquisition was planned to include intersecting traversal paths, thereby enhancing spatial referencing. Furthermore, each survey loop was designed to return to its point of origin, creating a closed-loop trajectory that improves the robustness of the SLAM solution. Post-acquisition, the raw trajectory data were processed into georeferenced point clouds using the GeoSLAM Hub software (version 6.0.0). The output was stored in the LAZ format. Tree detection and the estimation of stem curve, height, diameter, and volume were performed using an automatic algorithm developed by Hyyppä et al. (2020a,b). The algorithm was set to detect trees with a threshold value of 7 cm. To identify and analyse tree defects, the study employed the algorithm developed by Sagar et al. (2025), seamlessly complementing the earlier tree detection and measurement process.

Fig. 3. The ZEB Horizon LiDAR scanner integrated into a backpack-mounted mobile mapping system, equipped with a camera for geospatial data collection in forested environments. The entire setup weighs approximately 4 kg, making it portable for field use. Image © Ville Kankare.

Since the Zeb Horizon lacks a GNSS receiver, we georeferenced the tree maps as follows: First, the maps were aligned side by side by identifying and matching overlapping points. Once aligned, the maps were manually georeferenced to their real-world coordinates (ETRS-TM35FIN) using an orthoimage. After completing the spatial alignment, the focus shifted to cleaning and refining the dataset. Duplicate points at the same location were removed through a buffering process with a radius of 0.5–0.6 m. Overlapping points were dissolved, and the centroids of these dissolved geometries were extracted, resulting in a clean set of unique points representing the study area. Next, the area covered by the dataset was calculated. The boundaries enclosing the points were delineated, and the total area of the plots was computed. The points within each plot were extracted, enabling plot-level analysis. For each plot, the number of trees, their volume, average height, and basal area were determined, creating a comprehensive dataset for further ecological and forestry studies.

We also developed a custom map testing application (MapApp) using the C# programming language and the ThinkGeo map engine (ThinkGeo (2025), Frisco, Texas, United States), which enabled us to analyse and visualise tree maps for each forest stand.

2.3. Harvesting quality

2.3.1. Point clouds methods for observing tree defects

In this subsection, the primary focus is on deriving tree characteristics and identifying defects. The target tree defects are based on descriptions provided by Sagar et al. (2024, 2025). Defective trees were identified in the field; an example from Karstula site is shown in Fig. 4, and the point cloud data obtained from the MLS was post-processed using the following steps.

In step 1, the original point cloud data, captured to represent the entire forest area, was stored in the compressed LAZ format to manage the large file size, which exceeded 40 million (40,438,732) points in one forest stand. For visualisation and initial inspection, these LAZ files were opened using CloudCompare version 2.13.2 (Kharkiv - Jul 6, 2024) (CloudCompare), a 3D point cloud processing software, and then converted into the PCD (Point Cloud Data) format for compatibility with Python-based processing workflows using Python version 3.7. In step 2, the PCD file is loaded and read using the Python code, and the entire point cloud is visualised (Fig. 5a). The point clouds were spatially filtered by applying a proximity threshold, determined empirically through visual inspection, around the target tree coordinates obtained from the field survey using GPS measurements. Only points falling within the specified distance of the target trees were retained, resulting in a final dataset of almost 800,000 (790,395) points (Fig. 5b). This refined subset formed the basis for all subsequent processing and analysis, enabling focused investigation while preserving the structural integrity of the data relevant to the target trees.

Following the processing steps outlined in Sagar et al. (2025), step 3 involves removing ground (terrain) points (Fig. 5c), which isolates the ground points. Step 4 includes clustering and stem (tree) validation, where clusters are visually inspected (Fig. 5d) and branches and vegetation are filtered out if present. Step 5 focuses on analysing and assessing the structural properties of the stems. For each identified tree cluster, key structural characteristics are extracted to describe its geometry. These include the Central Position, calculated as the mean of the x- and y-coordinates of the point cloud, representing the horizontal location of the stem base, and Height, determined by the vertical extent of the tree, computed as the difference between the maximum and minimum z-values. These attributes form a basic description of each tree's size and spatial position, serving as essential inputs for further structural or ecological analysis. Additionally, DBH and maximum stem curve values are measured. The curvature value indicates stem defectiveness, providing a quantitative measure to assess whether the stem deviates from a typical, healthy form. Step 6 involves dividing the tree stem into sections as described in Sagar et al. (2024), with a centre line drawn between the upper and lower sections of the stem (Fig. 5e). For analysing the tree stem, a method is introduced to compute and visualise a laterally shifted centre line, based on the radius and primary orientation of the stem. This process involves several computational steps. First, an offset vector is derived — computed to be perpendicular to the stem's principal axis within the XY plane — ensuring the displacement is orthogonal to the vertical growth direction. This vector forms the basis for the next step, where it is scaled by the stem's radius and used to shift the original bottom and top points of the centre line. The result is a pair of new, spatially displaced endpoints that maintain the vertical extent but are laterally offset. These points are then connected to form a new centre line, representing a radial displacement from the original axis. Finally, this shifted geometry is visualised using Open3D (Fig. 5f), enabling intuitive visualisation of the modified centre line in relation to the original stem and branch point clouds. This visualisation aids in spatial interpretation and supports further structural analysis. Step 7 utilised the Open3D visualiser to display the output at each stage.

To evaluate the sensitivity of the algorithm and the overall system, the following procedure was implemented: Step 8, the Point Cloud was down-sampled. Given the substantial volume of data, a two-step reduction approach was employed to optimise computational efficiency. First, a random downsampling from a uniform distribution was performed using Python, retaining only 70 % of the original points. This reduced the dataset from over 40 million points to approximately 28 million (28,307,112) points, significantly decreasing the processing burden. The earlier steps 1–7 were rerun for the down-sampled data. The analysis resulted in the identification of eight trees, representing a reduction of one compared to the nine detected in the full point cloud processing. Despite this minor discrepancy, the method performed reliably: defective trees were accurately detected, and measurements were obtained in accordance with the protocol described by Sagar et al. (2025).

2.3.2. Strip road characteristics

This stage of the study involved mapping the strip roads within the study area (Fig. 6). This task required careful examination of harvester GNSS routes, open spaces, orthophotos, and hillshade maps. Once the strip roads were visually identified and delineated, the v.veronoi.skeleton GRASS processing tool was employed to generate a midline along each strip road (Fortune, 1987; OSGeo n.d.; Kotsur and Tereshchenko, 2019). This midline served as a crucial reference for creating a final line bisecting the strip roads. To enhance precision, points were placed every 10 m along this midline, laying the foundation for a detailed spatial network. With these reference points established, inter-distance lines were generated to analyse spatial relationships between strip roads. The

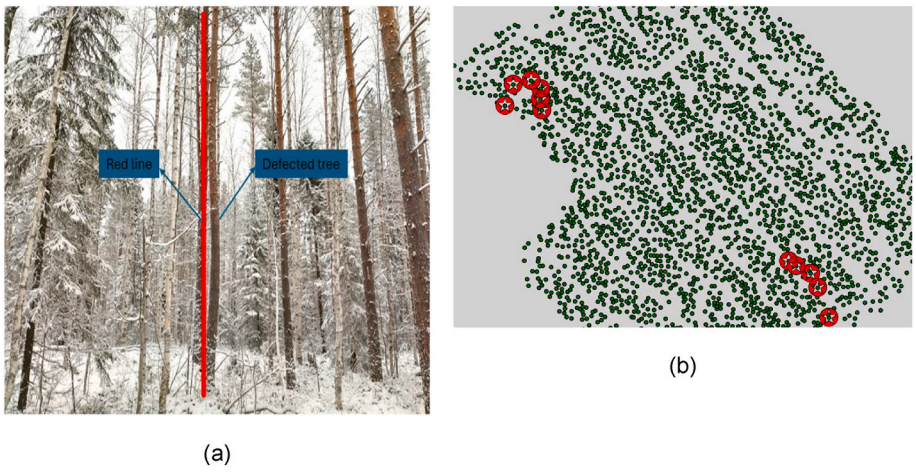

Fig. 4. Defected tree representation. (a) A defective tree within the forest stand. The red line is used to illustrate the curvature of the stem. (b) Tree map of a forest stand in Karstula. Each point represents an individual tree. Defective trees are highlighted with red stars.

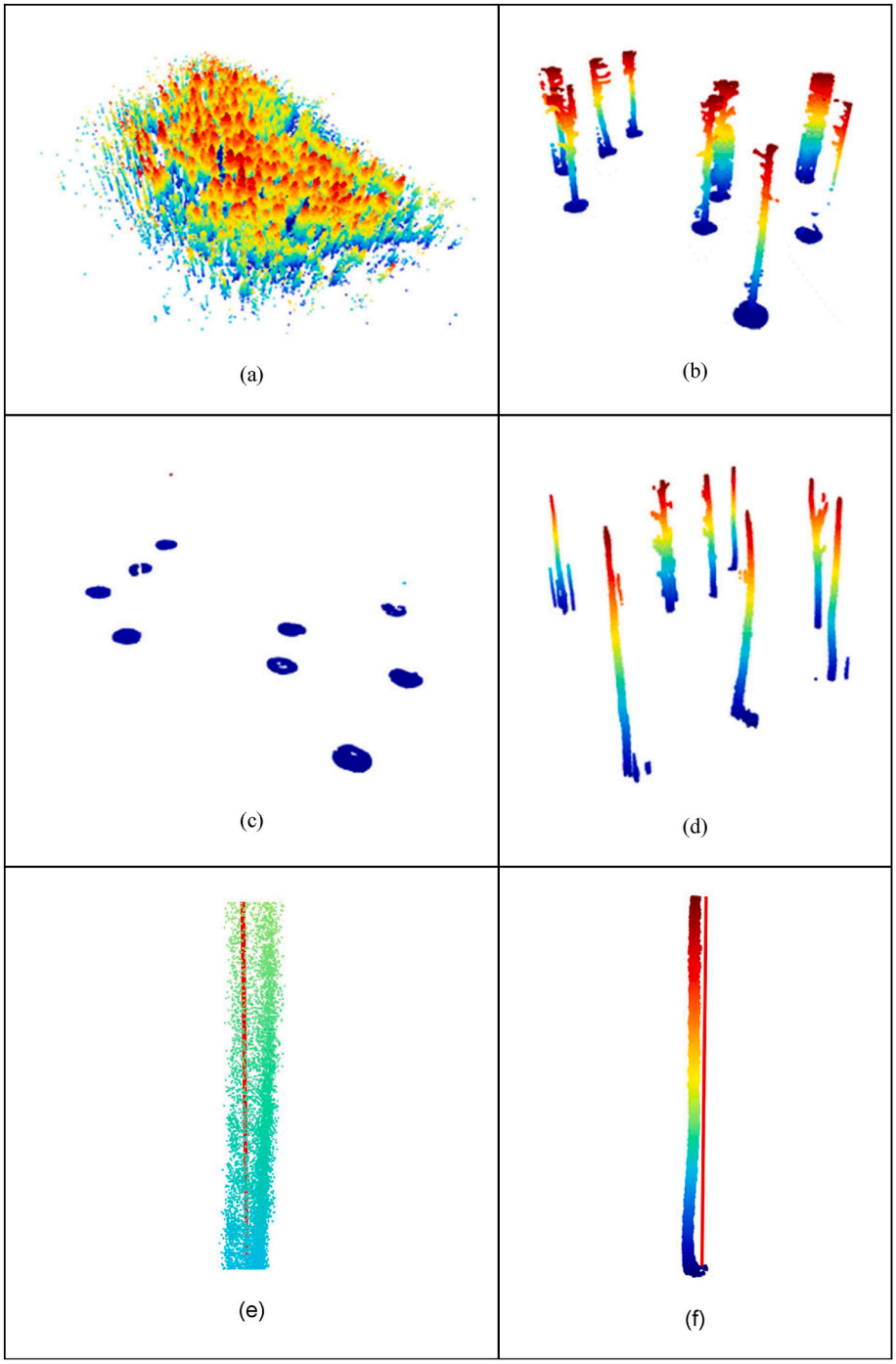

Fig. 5. Point cloud process. (a) Full input point cloud. (b) Filtered point cloud based on a set of predefined target tree coordinates. (c) Only the ground from the target trees. (d) filtered tree stems with some branches and vegetation. (e) Fine-tune the filtered tree stems so no more branches, tree stem with a straight line coloured in red, visualising the curved stem. (f) The stem with the shifted centre line in red colour, visualising the curved stem.

creation of inter-distance lines followed a methodology adapted from an online resource (Babel, 2020). For inter-distance lines, the (Join Attributes by Nearest) tool in QGIS was employed. Points along the 10-m intervals of one strip road were selected as the input layer, and the corresponding points from the next strip road were used as the target layer. This systematic approach ensured that the spatial relationships between features were accurately captured. QGIS's buffer processing tool was used to measure strip road width at intervals of 3, 3.5, 4, 4.5, and 5 m. The stems that intersected these buffers were selected, and the count of stems was divided by the length of the strip road.

The same buffer processing tool was also used to create a 16.92 m buffer along each strip road, determined by the minimum strip road spacing to prevent overlap between buffer zones. These topographically bounded areas were used to calculate stand details, ensuring that reference and MLS measurements cover the same area, and the possible impact of TDA on these areas is unambiguous.

2.4. Statistical analysis

The parametric *t*-test was utilised to determine whether the method of data collection influences the indicators of thinning quality. Additionally, the *t*-test was employed to assess whether operator guidance

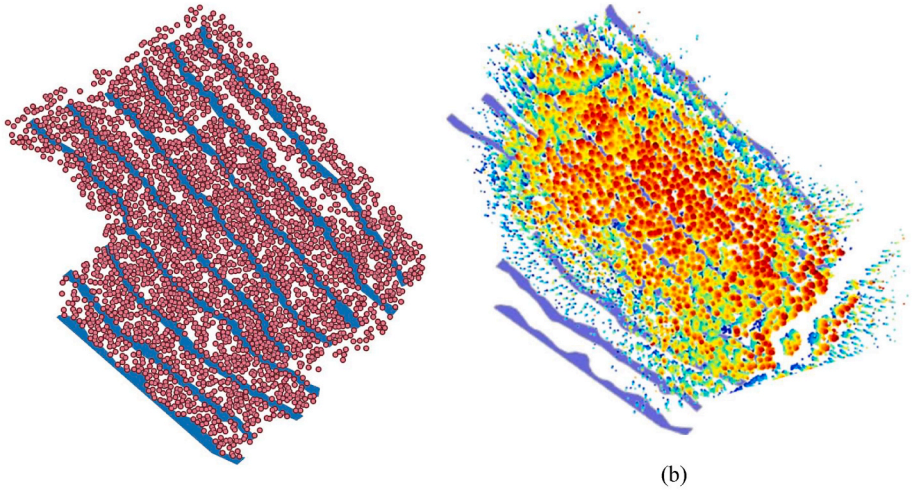

(a) (b)

Fig. 6. Strip road representation. (a) Tree map representation of a forest stand (Karstula site) on MapApp, showing strip roads. Red dots indicate the locations of trees, and blue lines depict the strip roads. (b) original point cloud with the fitted strip road highlighted in blue lines.

(TDA) impacts the thinning quality indicators collected through both traditional methods and MLS. A significance level of $\alpha \leq 0.05$ is used as a threshold for determining statistical significance. The t-statistic is given by

$$t = \frac{\underline{d}}{sd/\sqrt{n}} \tag{2}$$

Where $\underline{d}$ denotes the mean difference between two groups, *sd* standard deviation of the difference, *n* is the number of observations, and $sd/\sqrt{n}$ the standard error of the mean difference.

The accuracy of the MLS-derived estimates relative to the reference field data across all stands was evaluated using the root-mean-square error (RMSE), the percentage root-mean-square error (RMSE%), and bias for each structural variable. RMSE and RMSE% measure the prediction error, while bias and bias% quantify the systematic error. They are given as follows

$$RMSE = \sqrt{\frac{1}{n}\sum_{i=1}^{n}\left(x_i^{MLS} - x_i^{ref}\right)^2} \tag{3}$$

$$RMSE\% = \left(\frac{RMSE}{mean(x)}\right) \times 100 \tag{4}$$

$$Bias = \frac{1}{n}\sum_{i=1}^{n}\left(x_i^{MLS} - x_i^{ref}\right) \tag{5}$$

$$Bias\% = \left(\frac{Bias}{mean(x)}\right) \times 100 \tag{6}$$

Where *n* is the number of observations, x_i^{MLS} and x_i^{ref} values obtained from MLS and the corresponding reference field data value, respectively, for the *i*-th observation. The $mean(x)$ is the mean of the reference field data values.

The statistical tests, analyses, and figures were generated using the R programming language (R Core Team, 2025), utilising the *ggplot2* library for creating individual plots and the *gridExtra* for arranging multiple *ggplot* objects into a single composite figure. We used linear regression analysis, applying a transformation to the second power to model the strip road width. Multicollinearity issues were avoided by selecting only one buffer width (5 m in this case) as an explanatory variable, which was chosen based on the lowest p-values.

3. Results

3.1. Stem density

Stem density estimates derived from MLS generally exhibit lower mean and median values compared to reference measurements (ref) in stands 3 and 4 (Fig. 7 and Table 2). In stands 1 and 2, MLS estimates align more closely with the reference data. In stand 4, MLS slightly underestimates stem density, but with low error and no statistical significance, indicating good agreement with the reference. This pattern suggests a tendency of the MLS method to underestimate stem density, especially in young stands and structurally diverse plots, such as stand 3. However, the only statistically significant difference of 126 stems ha^{-1} between the reference density and MLS density ($t = 3.39$, $p < 0.01$) was observed in stand 3. In stand 1 – First thinning with slightly larger trees (~17 cm DBH) – the estimates were more consistent with the reference. The overall results showed that the RMSE of the stem density estimate was 113.1 m (19.9 %) and bias −9.7 (−1.7 %).

3.2. Basal area (G)

Basal area estimates from MLS broadly follow the trends of the reference measurements (Table 3 and Fig. 7). MLS slightly overestimates G, especially in stands 2 and 4, compared to the reference data, while in stands 1 and 3, estimates are much closer to each other. Despite these discrepancies, the overall interquartile ranges are reasonably consistent, though MLS estimates show fewer outliers. Statistically significant differences were observed only between the conventional and MLS methods on stand 2. These results imply a moderate agreement between MLS-derived and field-based G values, with some over-estimation depending on stand structure. Basal area LiDAR estimates are consistent in both first and later-thinning stands. The overall results showed that the RMSE of the G estimate was 3.1 m^2 (20.0 %) and the bias was 1.5 m^2 (9.7 %).

3.3. Dominant height

Among the six parameters, mean tree height exhibits the highest level of agreement between MLS-derived and reference data (Table 4 and Fig. 7). No statistically significant differences were found between the conventional and MLS methods. Medians and interquartile ranges are nearly identical in all four stands, with minor differences in stand 1. This suggests that MLS provides reliable and consistent estimates of

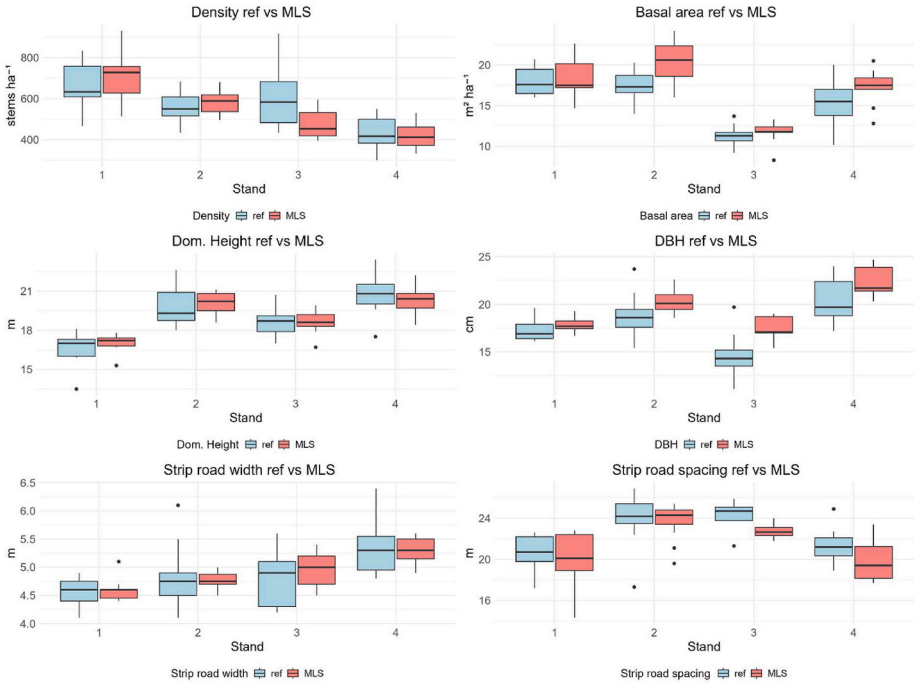

Fig. 7. Box plots illustrate the distribution of six key forest structural parameters across four forest stands (1–4), stem density (stems/ha), basal area (G, m^2/ha), dominant mean height (Dom. mean height, m), DBH (cm), strip road width (m) and strip road spacing. Each parameter is shown based on two data sources: reference field data (ref) and MLS point cloud-derived estimates.

Table 2
Statistical comparison of stem density (trees ha^{-1}) measurement data between reference (ref) and mobile laser scanning (MLS) across four forest stands; corresponding p-values from paired t-tests assessing the significance of methodological differences of measurement methods are shown in the last column.

Stand	Mean ref (trees ha^{-1})	Mean MLS (trees ha^{-1})	RMSE	RMSE-%	Bias	Bias-%	p-value
1	659	699	133.2	20.2	39.6	6.01	0.35
2	556	586	82.9	14.9	29.1	5.2	0.18
3	604	477	164.7	27.3	−126.4	−20.9	<0.01**
4	437	419	47.8	10.9	−18.1	−4.1	0.28
Overall	567	557	113.1	19.9	−9.7	−1.7	0.57

Table 3
Statistical analysis of basal area (G) measurements by stand. Mean ref and Mean MLS are in m^2 ha^{-1}. RMSE and bias are given in m^2 ha^{-1} and as percentages (%). p-values indicate the significance of differences between MLS and reference measurements.

Stand	Mean ref (m^2 ha^{-1})	Mean MLS (m^2 ha^{-1})	RMSE	RMSE-%	Bias	Bias-%	p-value
1	18.0	18.5	2.5	13.9	0.4	2.27	0.61
2	17.5	20.4	4.0	22.6	2.9	16.7	<0.01**
3	11.4	11.7	1.3	11.1	0.3	2.4	0.54
4	15.4	17.3	3.3	21.5	1.9	12.4	0.08
Overall	16.0	17.5	3.1	19.3	1.5	9.7	<0.001***

Table 4
Statistical analysis of dominant height measurements by stand. Mean ref and Mean MLS are in meters (m). RMSE and bias are reported in meters and as percentages (%). p-values indicate the significance of differences between MLS and reference measurements.

Stand	Mean ref (m)	Mean MLS (m)	RMSE	RMSE-%	Bias	Bias-%	p-value
1	16.6	17.0	0.8	4.7	0.4	2.5	0.07
2	19.8	20.1	1.1	5.4	0.2	1.1	0.43
3	18.7	18.7	0.6	3.5	−0.01	−0.1	0.96
4	20.7	20.3	1.5	7.3	−0.4	−2.1	0.42
Overall	19.0	19.1	1.0	5.5	0.1	0.5	0.57

dominant height, making it a robust variable for characterising forest structure in both first and later thinnings. The overall results showed that the RMSE of the dominant height estimate was 1.0 m (5.5 %), and the bias was 0.1 m (0.5 %).

3.4. Diameter at breast height (DBH)

Standwise, the MLS estimates were statistically significantly 0.6–2.5 cm larger than those measured as reference. The greatest variation was observed in stand 3, which had the smallest trees in this study (mean DBH 14.8 cm). Despite this statistical difference, the MLS demonstrates strong consistency with the reference data, closely matching the medians and interquartile ranges in all stands. In stand 1, there is a statistically significant difference of 0.7 cm between the reference (ref) and MLS-derived DBH ($t = -2.35$, $p < 0.05$). Similarly, stand 2 shows a statistically significant difference of 1.6 cm between DBH ref and DBH MLS ($t = -2.944$, $p < 0.05$). Stand 3 has the smallest and least variable DBH, indicating a younger stand, with a significant difference of 2.5 cm between DBH ref and DBH MLS ($t = -2.80$, $p < 0.05$). In stand 4, both data sources show the highest values and variability, indicating a stand with larger and more heterogeneous trees. Here, the statistically significant difference is 0.9 cm between DBH ref and DBH MLS ($t = -3.70$,

$p < 0.01$). For smaller diameter trees, such as in stand 3, the accuracy of diameter estimation is not particularly high. However, in stand 1, where trees approach a diameter of approximately 18 cm, the accuracy improves significantly. In the later thinning stand 4, where tree sizes vary, the estimation of average diameter is less accurate compared to the more uniform stand 2. Overall, the results showed that the RMSE of the DBH was 2.5 cm (13.9 %) and bias was 1.6 cm (8.9 %) (Table 5 and Fig. 7).

3.5. Strip road width

Overall, MLS performs well in estimating strip road width, with minor differences in variability and median values across the stands (Table 6 and Fig. 7). There were no statistically significant differences between reference and MLS estimates. Stand 3 exhibits the greatest variability in reference data, while MLS estimates show a more constrained range. Stand 4 consistently shows wider strip roads in both datasets. The overall results indicate that the RMSE of the strip road width was 0.4 m (8.47 %) and bias 0.01 m (0.1 %).

Determining the width of the strip roads required testing new methods. In the regression analysis, the number of trees per m within the 5-m buffer zone was selected as a predictor variable, alongside the density of remaining trees (see Table 7 and Fig. 7). The regression model has a moderate fit, explaining 41 % of the variance in the dependent variable with an average deviation of 0.41 m from the field-measured values. Fig. 8 illustrates the conceptual strip road layout, buffer-based width calculation, and potential midline detection errors.

3.6. Strip road spacing

MLS-derived values showed good alignment with reference measurements (Table 8 and Fig. 7). All stands follow a similar trend in both datasets, with stands 2 and 3 having the widest spacing and stand 1 the most variable. MLS data slightly underestimates the maximum, as the bias was −1.5 %–7.2 %, but effectively captures the central tendency and variability. A few outliers in both datasets suggest some irregularities due to terrain, obstacles, or harvesting constraints. In stand 4, there is a statistically significant difference of 1.2 m in strip road spacing ($t = 2.50$, $p < 0.05$). The overall results indicated that the RMSE of the strip road width was 1.5 m (6.9 %), and the bias was −0.8 m (−3.4 %).

3.7. Harvesting quality outcomes

TDA did not have a statistically significant effect on the harvesting quality attributes, regardless of whether they were measured using traditional methods (reference) or MLS technology. The results are presented in Appendix A (Tables A.1, A.2, A.3 and A.4). However, the different methods in some cases led to different conclusions. On stand 2: only G ref was under the recommendation, but over when measured with MLS. Stand 3: Both basal area measurements (G ref and G MLS) were slightly under the recommended, and the strip road width exceeded the recommended 4.5 m limit. Based on these results, only the thinning of the stand 3 – birch-dominated first thinning – resulted in an approximately 1 m^2 lower basal area than recommended (Table A.3). Additionally, in stand 3, located on mineral soil, the strip road width exceeded the recommended target of 4.5 m or less by 0.3 m in both treatments (Ref and TDA). In contrast, in stand 1, which was situated on peatland where the recommended width is 5 m (Leivo et al., 2023), the requirement was met in both treatments (Table A.2).

The recommended minimum spacing of 20 m between strip roads was met in all stands when measured using conventional methods and treatments (Ref or TDA). In the TDA plots, the strip road spacing was 0.2 m below the recommended spacing in stand 1 and 1.0 m below the recommended spacing in stand 4. The average of harvesting damages was below the recommended 5 % (Leivo et al., 2023), both in reference (1.9 %) and TDA plots (2.3 %). TDA did not have an effect on harvesting damages ($t = -0.56$, $p = 0.58$). The average harvesting intensity was slightly lower on TDA plots (0.5 on reference plots and 0.45 at TDA plots) but fell short of statistical significance ($t = 1.554$, $p = 0.128$)

Table 5
Statistical analysis of DBH at (1.3 m) measurement by stand. Mean ref and Mean MLS are in centimetres (cm). RMSE and bias are reported in centimetres and as percentages (%). p-values indicate the significance of differences between MLS and reference measurements.

Stand	Mean ref (cm)	Mean MLS (cm)	RMSE	RMSE-%	Bias	Bias-%	p-value
1	17.2	17.9	1.1	6.2	0.7	3.7	<0.05*
2	18.7	20.3	2.6	13.6	1.6	8.4	<0.05*
3	14.8	17.3	3.5	23.9	2.5	16.9	<0.05*
4	20.4	22.3	2.4	11.7	1.9	9.3	<0.01**
Overall	17.9	19.5	2.5	13.9	1.6	8.9	<0.001***

Table 6
Statistical analysis of strip road width measurement by a stand. Mean ref and Mean MLS are in meters (m). RMSE and bias are reported in meters and as percentages (%). p-values indicate the significance of differences between MLS and reference measurements.

Stand	Mean ref (m)	Mean MLS (m)	RMSE	RMSE-%	Bias	Bias-%	p-value
1	4.6	4.6	0.4	8.1	0.02	0.4	0.88
2	4.8	4.8	0.5	10.3	−0.1	−1.3	0.65
3	4.8	5.0	0.4	7.5	0.1	2.8	0.30
4	5.4	5.4	0.4	6.5	−0.06	−1.1	0.70
Overall	4.9	4.8	0.4	8.5	0.00	0.1	0.97

Table 7
Statistical information on the strip road width model (m). Independent variables are stem count (trees m^{-1}) in a 5 m range of the centre of the strip road and density of remaining trees (trees ha^{-1}).

Coefficient	Estimate of Coefficient	Standard Error of	t-value	Significance
Intercept	6.15	0.39	15.589	<0.001***
Stem count	11.53	3.74	−3.084	<0.01**
Stem count^2	29.34	11.51	2.549	<0.05 *
Density	0.000834	0.00089	−0.937	0.36

$R^2 = 0.41$, RSE 0.41, $F = 8.41$*** on 3 and 33 DF.

4. Discussion

4.1. Evaluation of study data and methods

The sample representativeness in field sample plots is crucial for accurately describing the population. According to Kangas et al. (2011), the internal variation within the population must be considered to ensure the reliability of the sample. The high number of systematically located circular sample plots ensured a representative sample in this study. Due to time constraints, it was not feasible to measure every tree on a circular plot. Nevertheless, this method provided a reliable estimate for DBH (Niemistö, 1992). Basal area was measured using a relascope from the centre of the circular plots. The relascope sample is commonly used in operational forest management, because it is fast but potentially more prone to errors, for example, due to visibility conditions and human errors (Haara and Korhonen, 2004; Kangas et al., 2004). DBH measurements of all trees on the circular sample plots could have been used to estimate not only DBH but also the basal area. The circular sampling plots were not measured between the strip roads to ensure that the specific tree was precisely within the TDA or reference area, while thinning in the border area of plots may have also been performed from the adjacent strip road. This was taken into account in both the MLS and

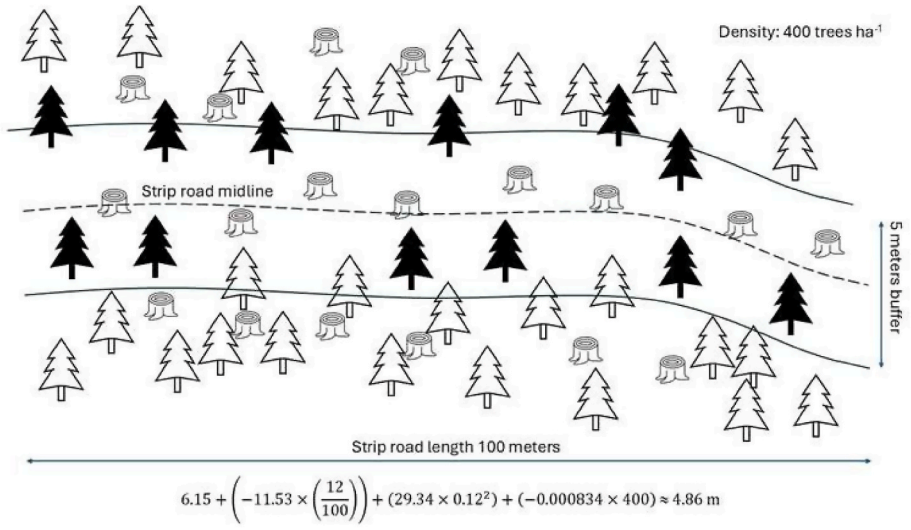

(a)

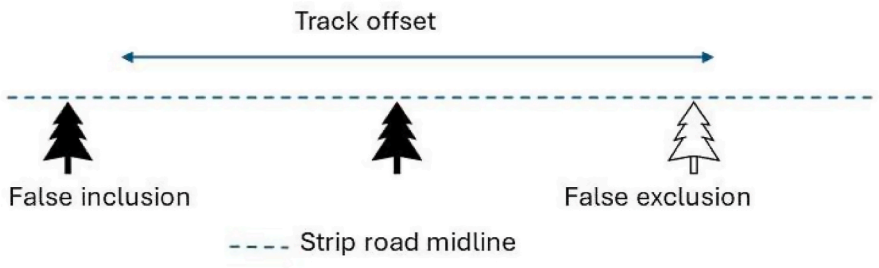

(b)

Fig. 8. Conceptual illustration of a strip road layout within a managed forest stand. Counted trees are coloured black, while other trees and stumps are white. (a) The strip road midline is marked with a dashed line, and the 5-m buffer zone (2,5 m on both sides of the strip road) is highlighted by solid blue lines. The mathematical calculation illustrates the application of the model under conditions where the strip road is 100 m long, the buffer contains 12 trees, and the residual stand density is 400 trees per hectare, resulting in a strip road width of 4.86 m. (b) Zoomed-in example of potential detection errors, such as GNSS offset or another midline position error caused by SLAM or the researcher.

Table 8
Statistical analysis of strip road spacing measurement by stand. Mean ref and Mean MLS are in meters (m). RMSE and bias are reported in meters and as percentages (%). Paired t-tests were performed for each spacing method (Ref and MLS) within each stand; corresponding p-values from *t*-test are shown in the final column. P-values indicate the significance of differences between MLS and reference measurements.

Stand	Mean ref (m)	Mean MLS (m)	RMSE	RMSE-%	Bias	Bias-%	p-value
1	20.4	20.0	1.1	5.2	−0.5	−2.4	0.17
2	24.1	23.7	1.3	5.2	−0.4	−1.5	0.31
3	24.0	22.5	2.1	8.6	−1.4	−5.7	0.22
4	21.1	19.9	2.1	10.0	−1.5	−7.2	<0.05*
Overall	22.4	21.7	1.5	6.9	−0.8	−3.4	<0.01**

reference measurements.

The tree maps and their associated data were then combined and georeferenced manually using an orthoimage. This step was labour-intensive, and the estimated time spent on each significant manual correction step is shown in Appendix B. This could have been avoided if the device had GNSS capabilities or if the tree maps had been registered to ALS tree maps (Hyyppä et al., 2021). By scanning only small areas at a time and using loop closures, we avoided the accumulating drift in the trajectory that arises in SLAM-based MLS operating without a reliable GNSS signal during long measurements (Faitli et al., 2024). However, loop closure is not possible in harvester-mounted systems, as the harvester or forwarder moves on the strip road and turns back only at the headlands of the stand. In this study, the Voronoi skeleton and segmentation tools were used to determine the centreline of the strip roads. Although useable, this method is labour-intensive. Alternatively, the centreline could be derived from the trajectory of a harvester equipped with a LiDAR sensor or by combining GNSS data with a georeferenced tree map. However, this method has limitations, including naturally stem-free areas and tree mortality, local stand structure and species composition, manual delineation and measurement error, and missing terrain parameters. More details are provided in Appendix C.

This study demonstrates that point clouds and tree maps can be used to assess harvesting quality. The tree map data collected by the harvester can be employed for long-term monitoring in the future. However, improvements are necessary, as the data must be collected and processed in real-time during cutting to prevent extremely large point clouds, and tree information such as diameter, height, and basal area should be displayed to the operator during harvesting.

4.2. Capability of point cloud data in detecting defects in individual trees (RQ1)

In alignment with the workflow outlined by Sagar et al. (2025) and utilising the same tree detection algorithm, we correctly identified 9 of

the 11 target trees, achieving a detection rate of 81.82 %. The two undetected individuals were likely missed due to a combination of partial canopy concealment by larger neighbouring trees, reducing their structural visibility in the point cloud, and potential suboptimal parameter settings within the detection algorithm. Notably, all trees exhibiting defects were accurately identified and measured, underscoring the strong potential of point cloud data for defect detection at the individual tree level. To supplement the limited number of naturally occurring defective trees in the study area (n = 11), the defect-detection component was also assessed using the set of simulated stem defects introduced and validated in our previous publication (Sagar et al., 2025). The small number of real defects reflects recent thinning operations carried out in the stand, during which most poor-quality or damaged trees had already been removed. As a result, the empirical sample was limited, and the simulated defects offered a necessary and previously verified basis for evaluating model behaviour across a wider range of defect conditions.

The primary limitation, therefore, lies not in classification accuracy but in the completeness of tree identification. When the point cloud was down-sampled to 70 % of its original density, detections decreased to 8 trees (72.73 %), yet all detected trees were again measured and defect-classified correctly. This indicates that while reduced point density can lower detection rates, it does not necessarily compromise defect assessment accuracy within the detected subset. Potential improvements include multi-angle scanning to reduce occlusion and refined segmentation to better resolve subtle crown structures. These omissions represent missed rather than false detections. Importantly, studies employing terrestrial laser scanning have demonstrated that dense point cloud data can reliably capture both log geometry and wood quality attributes in standing trees (Murphy et al., 2010; Pyörälä et al., 2019). This supports our finding that high-resolution MLS data provides a robust foundation for defect detection, even with varying point densities. This paves the way for stem quality guidance, which is considered one of the most valued future visions for operator support (Kärhä et al., 2021; Kymäläinen et al., 2024).

4.3. Consistency and reliability of MLS point cloud data in measuring harvesting quality across thinning stages (RQ2)

The overall results showed that the RMSE of the stem density estimate was 113 stem ha^{-1} (20.0 %), and the bias was −10 stem ha^{-1} (−1.7 %). Surprisingly, tree densities on stands 1 and 2 were slightly higher when measured using the MLS method compared to the field reference measurements. This finding was somewhat unexpected, as in results of Hyyppä et al. (2020a,b), automatic tree detection identified 93 % of trees in the sparse plot and only 77 % of trees in the more obstructed boreal forest plot. Possible explanations for achieving high accuracy in this study may lie in the systematic approach used in field measurements, in an even-aged and structurally uniform forest with a low proportion of spruce: 10 % in stand 1, 3 % in stand 2, 22 % in stand 3, and 24 % in stand 4, and with minimal undervegetation.

Hyyppä et al. (2020) faced significant challenges in identifying spruce trees, a problem also identified in this study. In stand 3, there was high variation in reference tree densities, as well as low tree detection in MLS. This stand (3) had a lot of trees with a diameter less than 10 cm, some of which were spruce. This seemed to pose a challenge for both real-time monitoring of thinning density (as TDA system) and post-analysis with an automatic tree detection algorithm developed and described by Hyyppä et al. (2020a,b), which discards possible trees if the stem curve can not be calculated. This is unfortunate because maintaining an adequate number of trees has been particularly challenging during the first thinnings (Finnish Forest Centre, 2023; Kotivuori et al. n. d.). The detection of small and low-branched trees requires different approaches, such as deep learning models (Henrich et al., 2024; Xiang et al., 2025).

The DBH estimates derived from MLS data demonstrated high agreement with reference measurements, yielding a low RMSE of 2.5 cm (13.9 %); however, there was a tendency to overestimate it by 1–2 cm (3.7–16.9 %). This level of accuracy is relatively high when compared to previous studies (Gollob et al., 2020; Hunčaga et al., 2020). With a bias compensation method, the most accurate laser scanning system based on a Velodyne VLP-16 sensor has achieved less than 10 % RMSE in an easy forest (Muhojoki et al., 2024). These studies are based on field measurements of individual trees. In contrast, the approach in this study utilised stand-wise estimation methods that achieved comparable precision for field use. These results underscore the reliability of MLS for assessing tree diameter distributions at the stand level, offering a robust alternative to more labour-intensive field-based techniques. Comparable accuracy to MLS can be achieved using a method based on (hpr) file. However, this method requires that the harvested trees closely match the remaining stand in terms of tree species composition and dimensional characteristics (Larsson, 2017; Strubergs et al., 2024).

Basal area estimates derived from MLS data were consistent with reference measurements. However, the MLS approach tends to overestimate basal area, with a bias of approximately 10 %. The observer-specific standard errors using relascope have been shown to range from 6.6 % to 24.5 % (Haara and Korhonen, 2004). Since basal area in the MLS method is calculated directly from individual tree diameters, the accuracy of DBH measurements has a direct impact on basal area estimation. In this study, the observed average DBH bias of less than 2 cm alone accounts for the 1–4 m^2 differences in basal area estimates between the methods, explaining the 10 % bias in basal area.

MLS point cloud-derived dominant height estimates demonstrated high agreement with conventional estimates, with a similar RMSE of 1.0 m compared to the 1–2 m RMSE observed by Hyyppä et al. (2020a,b) estimating individual tree heights. Based on the results, dominant height proves to be an excellent metric, even in MLS measurements, where the MLS enables the accurate calculation of tree height distribution profiles, stem profiles, and mean height. However, it is worth noting that when the MLS system is mounted on a forest harvester, its accuracy significantly decreases, as reported by Faitli et al. (2024). Dominant height is less sensitive to changes caused by thinning, especially low thinning, and reflects better the growth potential of trees compared to the arithmetic mean height (Tarmu et al., 2020). Moreover, dominant height can be estimated with high accuracy using ALS point clouds, with RMSE values as low as 0.8–0.9 m (Mehtätalo et al., 2015; Wang et al., 2019).

Strip road width using MLS was predicted using a regression model based on detected stems within a 5-m buffer from the centre line. This method can be considered relatively objective, as the estimates of the model did not show systematic deviation from reference measurements. However, deviations at the individual plot level were substantial, with an RMSE of 0.4 m. The accuracy is slightly better compared with the 0.6 m reported by Köppler (2017) using (hpr) file-based methods. However, the model still requires extensive testing and a significantly broader reference dataset. The approach is simple and could potentially be integrated into operator guiding systems Ponsse's TDA, and other equivalent systems in the future.

MLS-derived values for strip road spacing slightly underestimated the actual distance (by less than 1 m), but the overall results are promising. One possible explanation could be inaccuracies in the field measurements—particularly if the loggers tape did not cross the strip at its narrowest point or midpoint of strip road was wrongly determined, potentially resulting in slightly overestimated values. A key challenge in the method lies in defining the centreline of the strip road. In this study, the initial identification and delineation of the strip road edges were manually performed by the researcher. An automatic method utilising national ALS data has been proposed for the identification of strip roads (Abdi et al., 2022). Ponsse's TDA system already measures the distance to adjacent strip roads, although it currently does not log and save the data.

Even partial automation of thinning quality monitoring could significantly increase the amount of collected quality data while

simultaneously reducing monitoring costs for various stakeholders, such as forest companies, regulatory authorities and forest owners (Strubergs et al., 2024). However, devices like the Zeb Horizon, which rotate around their own axis, are not suitable for mounting on harvesters or forwarders due to demands for durability and robustness. Additionally, when the MLS system is mounted on the harvester, scanning is conducted along the strip road.

4.4. Impact of TDA system on harvesting quality outcomes (Q3)

The state-of-the-art TDA system is able to collect and visualise thinning density and strip road spacing data during forest operations, but at this stage, it did not show a statistically significant effect on harvesting quality (RQ3). With a few exceptions, values remained within the recommendations of Best Practice for Sustainable Forest Management (Leivo et al., 2023; Finnish Forest Centre, 2023). The damage percentage remained below the 5 % guideline, and the average thinning intensity was slightly lower in TDA plots (45 %) compared to reference plots (50 %), consistent with findings by Pohjala et al. (2024).

Study conditions likely influenced results, as operators were highly skilled (Purfürst, 2010), they may have worked more carefully than usual and often relied on personal judgement rather than TDA guidance. Limited prior experience with the system may also have reduced trust in its recommendations, while the cognitive load of machine operation and interpreting TDA input may have encouraged familiar decision-making over system-based guidance. Additionally, stand structure, species composition, and terrain conditions may have reduced the relative advantage of TDA recommendations.

Despite these limitations, the TDA shows promise as a stabilising tool for maintaining thinning density at prescribed target levels. By providing structured support, it can reduce operator reliance on intuition and lower the risk of deviations from silvicultural goals, especially for less experienced operators.

4.5. Future work

The point cloud data collected can be used to validate the simulation framework proposed by Sagar et al. (2025). It is important to note that this point cloud includes data on various tree properties beyond just curveness. While Sagar et al. focused solely on the curvature of the tree stem in their study, our research incorporates additional stem characteristics such as height and diameter at breast height (DBH). This real-world data can be utilised to simulate other forest properties beyond tree stem curvatures. In our analysis, we employed two algorithms, which can be compared using this dataset. Additionally, the data can be modified by introducing noise, adding or removing trees, or excluding strip roads, thereby enabling us to further validate the effectiveness of the algorithms.

Future studies should aim to increase the number of defective trees in the test dataset to enable stronger validation of our approach and a more thorough evaluation of the algorithm's robustness.

Additionally, research should explore the applicability of the TDA system in more complex forest environments, such as selectively harvested stands in continuous cover forestry (Korpunen et al., 2025), where operators cannot rely solely on visual assessment of stand density based on dominant height and tree species composition. In such settings, the ability of TDA in providing consistent and objective guidance may become more critical. Moreover, the effectiveness of the TDA could be strengthened by incorporating additional harvesting quality indicators beyond thinning density. This would expand its role from a supportive tool to a more comprehensive decision aid for both experienced and less experienced operators. Finally, since the present study was carried out in relatively simple stands where outcomes were straightforward, future studies should focus on more challenging stand and terrain conditions. These environments may reveal differences in performance, particularly when operators with limited experience rely heavily on TDA recommendations.

5. Conclusion

The findings reveal that MLS demonstrates strong potential for estimating key forest structural attributes, particularly stem density and dominant height, DBH, as well as strip road spacing and strip road width. Across most forest stands, MLS provided stem density estimates with acceptable accuracy; however, performance varied with stand complexity. In denser or structurally intricate environments, MLS consistently underestimated stem counts, highlighting a sensitivity to occlusion or vegetation clutter. This suggests that while MLS is effective under typical conditions, its performance may benefit from site-specific calibration in more challenging forest settings. In contrast, dominant height measurements derived from MLS showed a high degree of consistency and alignment with reference data. Bias across all stands remained minimal, and no statistically significant deviations were observed, affirming the robustness of MLS for capturing vertical structural characteristics. These results reinforce MLS as a reliable and scalable tool for forest inventory applications, including defect detection and the evaluation of harvesting quality. Although minor variations in accuracy were observed, they appear to be linked to local stand conditions rather than systematic errors, supporting the broader operational applicability of MLS in diverse forest environments.

CRediT authorship contribution statement

Anwar Sagar: Writing – review & editing, Writing – original draft, Visualization, Software, Methodology, Formal analysis, Data curation, Conceptualization. **Johannes Pohjala:** Writing – review & editing, Writing – original draft, Visualization, Software, Methodology, Formal analysis, Data curation, Conceptualization. **Jesse Muhojoki:** Writing – review & editing, Software, Formal analysis. **Anubhav Dhital:** Writing – review & editing, Formal analysis. **Harri Kaartinen:** Writing – review & editing, Data curation. **Kalle Kärhä:** Writing – review & editing, Supervision. **Kalervo Järvelin:** Writing – review & editing. **Reza Ghabcheloo:** Writing – review & editing, Supervision. **Juha Hyyppä:** Writing – review & editing, Supervision. **Ville Kankare:** Writing – review & editing, Writing – original draft, Supervision, Methodology.

Funding

This research was funded by Ponsse Plc and NextGenerationEU— European Union through “Nappaa hiilestä kiinni” program and the Ministry of Agriculture and Forestry (grant number VN/27353/2022 for IlmoStar).

Declaration of competing interest

The authors declare that they have no known competing financial interests or personal relationships that could have appeared to influence the work reported in this paper.

Acknowledgments

The authors would like to thank the following individuals for their generous support and assistance with this research: Juha Inberg, Pia Kauhanen, Panu Johansson, Tomi Piirainen, Joni Backas, and Mikko Haapalainen. They also thank the anonymous reviewers for their constructive feedback and suggestions.

Appendix A

Table A.1
Comparison of density (stem ha^{-1}) between field-based (Density Ref) and MLS-based (Density MLS) measurements. Values in brackets are the range values. Paired t-tests were performed for each method (G Ref and G MLS) within each stand; corresponding t- and p-values are shown in the final columns.

Stand	Treatment	Density ref (Stem ha^{-1})	t-value	p-value	Density MLS (Stem ha^{-1})	t-value	p-value
1	Ref	696 [600–833]	0.99	0.35	724 [665–781]	0.80	0.45
	TDA	628 [467–800]			674 [515–931]		
2	Ref	586 [517–683]	1.38	0.20	562 [507–639]	−1.41	0.18
	TDA	534 [533–616]			601 [497–680]		
3	Ref	654 [433–917]	0.8	0.46	486 [407–550]	0.3	0.77
	TDA	563 [450–717]			470 [332–530]		
4	Ref	450 [300–550]	0.8	0.45	417 [332–530]	−0.94	0.93
	TDA	421 [383–500]			421 [332–490]		

Table A.2
Comparison of strip road width (m) between treatments (Ref and TDA) using field-based (Width Ref) and MLS-based (Width MLS) measurements. The recommended target width is 4–4.5 m in first thinnings (Stands 1 and 3 in this study). Values in brackets are the range values. Paired t-tests were performed between treatment (Ref and TDA) within each stand; corresponding t- and p-values are shown in the corresponding columns.

Stand	Treatment	Width ref (m)	t-value	p-value	Width MLS (m)	t-value	p-value
1	Ref	4.6 [4.3–4.9]	−0.05	0.97	4.5 [4.4–4.6]	−2.33	0.05
	TDA	4.6 [4.1–4.8]			4.7 [4.5–5.1]		
2	Ref	4.8 [4.4–5.5]	−0.52	0.61	4.8 [4.5–5.0]	1.25	0.25
	TDA	4.9 [4.1–6.1]			4.7 [4.5–4.9]		
3	Ref	4.8 [4.3–5.1]	−0.26	0.80	5.0 [4.7–5.4]	0.16	0.88
	TDA	4.9 [4.3–5.6]			4.9 [4.5–5.3]		
4	Ref	5.5 [4.8–6.4]	0.98	0.36	5.4 [5.1–5.6]	−1.17	0.31
	TDA	5.2 [4.8–5.6]			5.2 [4.9–5.4]		

Table A.3
Comparison of basal area (m^2) between treatments (Ref and TDA) using field-based (G Ref) and MLS-based (G MLS) measurements. Values in brackets are the range values. Paired t-tests were performed between treatment (Ref and TDA) within each stand; corresponding t- and p-values of these tests are in respective columns. The recommended target basal area according to Best Practices for Sustainable Forest Management in Finland is shown in the final column.

Stand	Treatment	G ref (m^2)	t-value	p-value	G MLS (m^2)	t-value	p-value	G Best practice (m^2)
1	Ref	18.4 [17.0–19.6]	0.70	0.50	18.9 [17.4–20.6]	0.59	0.57	16.9
	TDA	17.7 [16.0–20.6]			18.1 [14.7–22.6]			16.7
2	Ref	16.9 [14.0–19.7]	−1.23	0.25	19.1 [16.6–22.9]	−1.80	0.10	18.0
	TDA	17.9 [15.8–20.3]			21.3 [16.0–24.2]			18.0
3	Ref	11.3 [9.2–12.8]	−0.19	0.86	11.3 [8.3–13.3]	0.65	0.56	13.5
	TDA	11.5 [10.7–13.7]			12.0 [11.7–12.4]			13.5
4	Ref	15.4 [10.2–20.0]	0.01	0.95	16.5 [12.8–20.5]	−1.36	1	14.5
	TDA	15.4 [13.3–17]			18.3 [17.2–19.3]			14.5

Table A.4
Comparison of strip road spacing (m) between treatments (Ref and TDA) using field-based (Spacing Ref) and MLS-based (Spacing MLS) measurements. The recommended target spacing is 20 m. Values in brackets are the range values. Paired t-tests were performed between treatment (Ref and TDA) within each stand; corresponding t- and p-values are shown in the corresponding columns.

Stand	Treatment	Spacing ref (m)	t-value	p-value	Spacing MLS (m)	t-value	p-value
1	Ref	20.9 [17.2–22.6]	0.59	0.58	20.2 [14.3–22.4]	0.59	0.57
	TDA	20.1 [17.6–22.3]			19.8 [17.5–22.8]		
2	Ref	23.4 [17.3–26.8]	−0.45	0.68	23.2 [19.1–25.0]	−0.58	0.68
	TDA	24.4 [22.4–26.9]			23.9 [21.1–25.4]		
3	Ref	24.7 [23.5–25.9]	1.0	0.46	23.4 [22.8–24.0]	2.21	0.17
	TDA	23.0 [21.3–24.6]			21.8 [21.2–22.5]		
4	Ref	21.5 [19.1–24.9]	0.66	0.53	21.1 [18.4–23.4]	1.28	0.29
	TDA	20.7 [18.9–21.5]			19.0 [17.6–21.0]		

Appendix B

Table B.1
Efficiency Analysis and Manual Correction Time in Tree Point Cloud Data Manual corrections within the tree point cloud workflow mainly involved georeferencing tree maps, cleaning and refining datasets, and validating through visual inspection. The following table summarises the estimated time spent on each significant manual correction step, based on experience from this study.

Manual Correction Step	Description	Estimated Time per ha
Georeferencing & Alignment	Aligning tree maps with orthoimages, matching overlapping points	60–120 min
Duplicate Removal & Cleaning	Removing duplicate points, buffering, and dataset refinement	40–60 min
Final Quality Check	Ensuring spatial accuracy, completeness, and data integrity	20–60 min
Total Estimated Time	Sum of all manual corrections per plot	120–240 min

Appendix C

Table C.1
Summary of key limitations, sources of uncertainty, and recommended methodological improvements affecting stem-based estimation of strip road width in forest stands.

Category	Description
Stem-Free Areas and Tree Mortality	The model does not account for naturally occurring canopy gaps, stem-free zones, or tree mortality, which can create irregular spacing unrelated to strip roads and bias stem-based width estimates.
Stand Structure and Species Composition	Variability in species composition, understory density, and the presence of suppressed or dead trees can reduce the reliability of stem counts, particularly in heterogeneous or complex terrain.
Manual Delineation Error	Subjective manual delineation of strip road boundaries introduces measurement error and researcher bias, contributing to unexplained model variance.
Terrain Effects	The absence of terrain variables (e.g., slope, elevation, soil type, microtopography) limits model performance, as terrain strongly influences strip road placement, geometry, and spacing.
Terrain Data Integration	Incorporating terrain data from DEMs or high-resolution remote sensing could improve model realism by accounting for both operational constraints and natural stand features.
Future Research Directions	Recommended improvements include integrating terrain parameters, applying automated strip road delineation methods, and expanding datasets to encompass diverse stand and terrain conditions.

Data availability

Data will be made available on request.

References

Abdi, O., Uusitalo, J., Kivinen, V.-P., 2022. Logging trail segmentation via a novel U-Net convolutional neural network and high-density laser scanning data. Remote Sens. 14 (2), 349. https://doi.org/10.3390/rs14020349.

Ahlgren, T., 1982. Mätning Av Skador i Gallring. Forskningsstiftelsen Skogsarbeten. Resultat nr 24.

Ampoorter, E., de Schrijver, A., van Nevel, L., Hermy, M., Verheyen, K., 2012. Impact of mechanized harvesting on compaction of sandy and clayey forest soils: results of a meta-analysis. Ann. For. Sci. 69, 533–542. https://doi.org/10.1007/s13595-012-0199-y.

Arlinger, J., Möller, J.J., Sorsa, J.A., Räsänen, T., 2021. Introduction to StanForD 2010: structural descriptions and implementation recommendations. Skogforsk. Available online: https://www.skogforsk.se/contentassets/1a68cdce4af1462ead048b7a5ef1cc06/stanford-2010-introduction-150826.pdf. (Accessed 20 September 2025).

Arvidsson, A., Knutell, H., 1977. Mekaniserad fällning gallring under vinterförhållanden. Skogshögsskolan, institutionen för skogsteknik. Rapporter och Uppsatser 120.

Babel, 2020. Creating perpendicular lines on line using QGIS. https://gis.stackexchange.com/questions/380361/creating-perpendicular-lines-on-line-using-qgis. (Accessed 20 September 2025).

Bauwens, S., Bartholomeus, H., Calders, K., Lejeune, P., 2016. Forest inventory with terrestrial LiDAR: a comparison of static and hand-held Mobile laser scanning. Forests 7, 127. https://doi.org/10.3390/f7060127.

Bergkvist, G., Staland, J., 2003. Gallra med kvalitet: förberedelser, utförande, uppföljning & återkoppling. Stiftelsen Skogsbrukets Forskningsinstitut. Available at https://www.skogforsk.se/contentassets/9281346e032e401faf7dd9dca6455d73/gallra-med-kvalitet.pdf.

Bettinger, P., Kellogg, L.D., 1993. Residual stand damage from cut-to-length thinning of second-growth timber in the Cascade range of Western Oregon. For. Prod. J. 43 (11), 59, 12.

Björheden, R., Fröding, A., 1986. Ny rutin för praktisk gallringsuppföljning. New routine for checking the biological quality of thinning in practice. Sveriges lantbruksuniversitet, Institutionen för skogsteknik. Uppsatser och Resultat 48.

Bucht, S., 1977. Vad kostar stickvägarna tillväxt? Summary: the influence of strip roads on increment at the first thinning in Scots pine forests. Skogen 6, 218–222.

Cajander, A.K., 1926. The theory of forest types. Acta For. Fenn. 29 (3), 7193. https://doi.org/10.14214/aff.7193.

Calders, K., Adams, J., Armston, J., Bartholomeus, H., Bauwens, S., Bentley, L.P., Chave, J., Danson, F.M., Demol, M., Disney, M., Gaulton, R., Krishna Moorthy, S.M., Levick, S.R., Saarinen, N., Schaaf, C., Stovall, A., Terryn, L., Wilkes, P., Verbeeck, H., 2020. Terrestrial laser scanning in forest ecology: expanding the horizon. Rem. Sens. Environ. 251, 112102. https://doi.org/10.1016/j.rse.2020.112102.

Cambi, M., Certini, G., Neri, F., Marchi, E., 2015. The impact of heavy traffic on forest soils: a review. Ecol. Manag. 338, 124–138. https://doi.org/10.1016/j.foreco.2014.11.022.

Cameron, A.D., 2002. Importance of early selective thinning in the development of long-term stand stability and improved log quality: a review, forestry. Int. J. Financ. Res. 75 (1), 25–35. https://doi.org/10.1093/forestry/75.1.25.

Carlestål, B., Dehlén, R., 1977. Gallringsmetoder för självverksamma skogsägare. Rapporter och uppsatser. Institutionen för Skogsteknik 105.

CloudCompare. https://www.cloudcompare.org/main.html. (Accessed 20 September 2025).

Di Stefano, F., Chiappini, S., Gorreja, A., Balestra, M., Pierdicca, R., 2021. Mobile 3D scan LiDAR: a literature review. Geomat. Nat. Hazards Risk 12 (1), 2387–2429. https://doi.org/10.1080/19475705.2021.1964617.

Diggle, P., Knutell, H., 1979. "Kniggle" – en ny metod för skattning av stickvägsbredd. Summary: "Kniggle" new Method for Estimating Strip Road Width. Sveriges lantbruksuniversitet, Institutionen för skogsteknik. Rapport 4.

Faitli, T., Hyyppä, E., Hyyti, H., Hakala, T., Kaartinen, H., Kukko, A., Muhojoki, J., Hyyppä, J., 2024. Integration of a Mobile laser scanning system with a Forest harvester for accurate localization and tree stem measurements. Remote Sens. 16, 3292. https://doi.org/10.3390/rs16173292.

Finnish Forest Centre, 2023. Ensiharvennuksissa moni metsä hakataan edelleen liian harvaksi – tilanne on kuitenkin parantunut viime vuosista [Press release]. https://www.metsakeskus.fi/fi/ajankohtaista/ensiharvennuksissa-moni-metsa-hakataan-edelleen-liian-harvaksi-tilanne-on-kuitenkin-parantunut-viime-vuosista.

Fortune, Steve J., 1987. A sweepline algorithm for voronoi diagrams. Algorithmica 2, 153–174. https://doi.org/10.1007/BF01840357.

GeoSLAM, 2025. ZEB Horizon RT Mobile Laser Scanner. FARO Technologies Inc. Retrieved from. https://www.faro.com/en/Products/Hardware/GeoSLAM-ZEB-Horizon-RT.

Gollob, C., Ritter, T., Nothdurft, A., 2020. Forest inventory with long range and high-speed personal laser scanning (PLS) and simultaneous localization and mapping (SLAM) technology. Remote Sens. 12, 1509. https://doi.org/10.3390/rs12091509.

Haara, A., Korhonen, K.T., 2004. Kuvioittaisen arvioinnin luotettavuus. Metsätieteen Aikakauskirja 4/2004, pp. 489–508.

Hannrup, B., Möller, J.J., Arlinger, J., Eriksson, I., 2021. Förbättrad styrning av gallringsarbetet för ökad tillväxt i yngre och medelålders skog. Arbetsrapport 1085–2021. Skogforsk 37. Available at https://www.skogforsk.se/contentassets/a3afa12f4be8477f980b91e2a6319525/1085-2021.pdf. (Accessed 20 September 2025).
Harstela, P., 1996. Forest Work Science and Technology. Part 2. Joensuun Yliopisto.
Henrich, J., van Delden, J., Seidel, D., Kneib, T., Ecker, A.S., 2024. TreeLearn: a deep learning method for segmenting individual trees from ground-based LiDAR forest point clouds. Ecol. Inform. 84, 102888. https://doi.org/10.1016/j.ecoinf.2024.102888.
Holmgren, J., Persson, Å., 2004. Identifying species of individual trees using airborne laser scanner. Rem. Sens. Environ. 90 (4), 415–423. https://doi.org/10.1016/S0034-4257(03)00140-8. ISSN 0034-4257.
Hunčaga, M., Chudá, J., Tomaštík, J., Slámová, M., Koreň, M., Chudý, F., 2020. The comparison of stem curve accuracy determined from point clouds acquired by different terrestrial remote sensing methods. Remote Sens. 12 (17), 2739. https://doi.org/10.3390/rs12172739.
Hyyppä, E., Kukko, A., Kaijaluoto, R., White, J.C., Wulder, M.A., Pyörälä, J., Liang, X., Yu, X., Wang, Y., Kaartinen, H., Virtanen, J.-P., Hyyppä, J., 2020a. Accurate derivation of stem curve and volume using backpack Mobile laser scanning. ISPRS J. Photogrammetry Remote Sens. 161, 246–262. https://doi.org/10.1016/j.isprsjprs.2020.01.018.
Hyyppä, E., Yu, X., Kaartinen, H., Hakala, T., Kukko, A., Vastaranta, M., Hyyppä, J., 2020b. Comparison of backpack, handheld, under-canopy UAV, and above-canopy UAV laser scanning for field reference data collection in boreal forests. Remote Sens. 12 (20), 3327. https://doi.org/10.1016/j.isprsjprs.2020.03.021.
Hyyppä, E., Muhojoki, J., Yu, X., Kukko, A., Kaartinen, H., Hyyppä, J., 2021. Efficient coarse registration method using translation- and rotation-invariant local descriptors towards fully automated forest inventory. ISPRS Open J. Photogrammetry Rem, Sens, 2, 100007. https://doi.org/10.1016/j.ophoto.2021.100007.
Iittiläinen, P., Hyppölä, A., Kariniemi, A., Nieminen, T., Poikela, A., Ranta, R., Roininen, K., Rumpunen, H., Tolonen, H., Äijälä, O., 2003. Korjuujälki harvennushakkuussa. Metsäteho. https://www.metsateho.fi/wp-content/uploads/2015/03/Korjuujalki_harvennushakkuussa_opas.pdf. (Accessed 20 September 2025).
Isomäki, A., 1994. Ajouran leveyden määritys. Summary: determination of strip road width. Metsantutkimuslaitoksen Tied. 501, 66. ISBN 951-40-1366-2, ISSN 0358-4283.
Isomäki, A., Kallio, T., 1974. Consequences of injury caused by timber harvesting machines on the growth and decay of spruce (Picea abies (L.) Karst.). Acta For. Fenn. (136), 7570. https://doi.org/10.14214/aff.7570.
Isomäki, A., Niemistö, P., 1990. Ajourien vaikutus puuston kasvuun Etelä-Suomen nuorissa kuusikoissa. Abstract: effect of strip roads on the growth and yield of young spruce stands in southern Finland. Folia For. 756, 36.
Kafle, B., Kankare, V., Kaartinen, H., Väätäinen, K., Hyyti, H., Faitli, T., Hyyppä, J., Kukko, A., Kärhä, K., 2025. Assessing the consistency of low vegetation characteristics estimated using harvester, handheld, and drone light detection and ranging (LiDAR) systems. Silva Fenn. 59 (2), 25013. https://doi.org/10.14214/sf.25013.
Kangas, A., Heikkinen, E., Maltamo, M., 2004. Accuracy of partially visually assessed stand characteristics: a case study of Finnish forest inventory by compartments. Can. J. For. Res. 34 (4), 916–930. https://doi.org/10.1139/x03-266.
Kangas, A., Päivinen, R., Holopainen, M., Maltamo, M., 2011. Silva Carelica 40. Metsänmittaus Ja Kartoitus. University of Eastern Finland, School of Forest Sciences, p. 210.
Kankare, V., Luoma, V., Saarinen, N., Peuhkurinen, J., Holopainen, M., Vastaranta, M., 2019. Assessing feasibility of the forest trafficability map for avoiding rutting – a case study. Silva Fenn. 53 (3), 10197. https://doi.org/10.14214/sf.10197.
Kärhä, K., Ovaskainen, H., Palander, T., 2021. Decision-making Among harvester operators in tree selection and need for advanced harvester operator assistant systems (AHOASs) on thinning sites. In: Chung, W., Sessions, J., Lyons, K., Wigginton, K. (Eds.), Proceedings of the Joint 43rdAnnual Meeting of Council on Forest Engineering (COFE)& the 53rd International Symposium on Forest Mechanization (FORMEC), Forest Engineering Family – Growing ForwardTogether, September 27–30, pp. 15–25. Corvallis, OR, USA.
Kellomäki, S., 2022. Management of Boreal Forests : Theories and Applications for Ecosystem Services. Springer. https://doi.org/10.1007/978-3-030-88024-8.
Köppler, L., 2017. Automatisk Gallringsuppföljning - Utvärdering Av Stickvägslängd Beräknad Från Skördarnas Produktionsdata. Master's Thesis. Swedish University of Agricultural Sciences, Umeå. SLU, p. 34.
Korhonen, L., Kärhä, K., Maltamo, M., Malinen, J., Hyyppä, J., Kaartinen, H., Toivonen, J., Packalen, P., Koivula, M., 2024. Remote sensing and forest machine sensors in monitoring forest biodiversity indicators. J. For. Sci. https://doi.org/10.14214/ma.23010 article 23010.
Korpunen, H., Nuutinen, Y., Jylhä, P., Eliasson, L., Granhus, A., Laitila, J., Hoffmann, S., Muhonen, T., 2025. Harvesting of continuous cover forests. In: Rautio, P., et al. (Eds.), Continuous Cover Forestry in Boreal Nordic Countries (Managing Forest Ecosystems, vol. 45. Springer. https://doi.org/10.1007/978-3-031-70484-0_6.
Kotivuori E., Hytönen H., Haataja, L. (n.d.). Perinteisten Korjuujäljen Tarkastusten Puustotunnusten Luotettavuus Koealaotannan Näkökulmasta (26 pages). Suomen metsäkeskus. Retrieved June 3, 2025. Available at: https://www.metsakeskus.fi/sites/default/files/document/korjuujaljen-tarkastusten-luotettavuus-smk.pdf. (accessed on September 20, 2025).
Kotsur, D., Tereshchenko, V., 2019. Optimization heuristics for computing the voronoi skeleton. In: Rodrigues, J., et al. (Eds.), Computational Science – ICCS 2019. ICCS 2019, Lecture Notes in Computer Science, vol 11536. Springer, Cham. https://doi.org/10.1007/978-3-030-22734-0_8.
Krishna Moorthy, S.M., Calders, K., Vicari, M.B., Verbeeck, H., 2020. Improved supervised learning-based approach for leaf and wood classification from LiDAR point clouds of forests. IEEE Trans. Geosci. Rem. Sens. 58 (5), 3057–3070. https://doi.org/10.1109/TGRS.2019.2947198.
Kymäläinen, H., Häggström, C., Hujala, T., Torssonen, P., Malinen, J., 2024. Ergonomics in CTL harvesting – assisting systems and future visions. Int. J. For. Eng. 36 (2), 133–146. https://doi.org/10.1080/14942119.2024.2438500.
Laajalehto, J., 2025. Skid Trails in Commercial Thinning: a Literature Review Major Essay, Master of Forestry. University of British Columbia.
Larsson, M., 2017. Precision i automatisk gallringsuppföljning. Arbetsrapport. UMEÅ: Sveriges lantbruksuniversitet.
Leivo, J., Partanen, J., Hytönen, H., Leppijoki, N., Pulkkanen, T., Haataja, L., Pirkonen, J., Partamies, M., Santapukki, R., Nousiainen, M., Pakkanen, N., 2023. Tarkastusohje [Inspection Guidelines]. Finnish Forest Centre. Available at https://www.metsakeskus.fi/sites/default/files/document/tarkastusohje.pdf.
Liang, X., Hyyppä, J., Kukko, A., Kaartinen, H., Jaakkola, A., Yu, X., 2014. The use of a mobile laser scanning system for mapping large forest plots. IEEE Geosci. Rem. Sens. Lett. 11 (9), 1504–1508. https://doi.org/10.1109/LGRS.2013.2297418.
Liang, X., Kankare, V., Hyyppä, J., Wang, Y., Kukko, A., Haggrén, H., Yu, X., Kaartinen, H., Jaakkola, A., Guan, F., Holopainen, M., Vastaranta, M., 2016. Terrestrial laser scanning in forest inventories. ISPRS J. Photogrammetry Remote Sens. 115, 63–77. https://doi.org/10.1016/j.isprsjprs.2016.01.006.
Liang, X., Kukko, A., Balenović, I., Saarinen, N., Junttila, S., Kankare, V., Holopainen, M., Mokroš, M., Surový, P., Kaartinen, H., Jurjević, L., Honkavaara, E., Näsi, R., Liu, J., Hollaus, M., Tian, J., Yu, X., Pan, J., Cai, S., Virtanen, J.-P., Wang, Y., Hyyppä, J., 2022. Close-range remote sensing of forests: the state of the art, challenges, and opportunities for systems and data acquisitions. IEEE Geosci. Rem. Sens. Magazine 10 (3), 32–71. https://doi.org/10.1109/MGRS.2022.3168135.
Lilleberg, R., 1984. Kasvatushakkuiden korjuujälki. Summary: the state of harvested thinning stands. Metsätehon tiedotus 388. Metsäteho.
Lilleberg, R., 1986. Harvennushakkuuleimikoiden korjuujälki kehittyneempiä menetelmiä käytettäessä. Summary: advanced harvesting methods and damage to residual growing stock. Metsätehon katsaus 12. Metsäteho.
Liu, Z., Kaartinen, H., Hakala, T., Hyyti, H., Hyyppä, J., Kukko, A., Chen, R., Vastaranta, M., 2025. Ultra-wideband-based method for measuring tree positions with decimeter-level accuracy under a forest canopy. IEEE J. Sel. Top. Appl. Earth Obs. Rem. Sens. https://doi.org/10.1109/JSTARS.2025.3569958.
Mehtätalo, L., Virolainen, A., Tuomela, J., Packalen, P., 2015. Estimating tree height distribution using low-density ALS data with and without training data. IEEE J. Sel. Top. Appl. Earth Obs. Rem. Sens. 8 (5), 2400–2408. https://doi.org/10.1109/JSTARS.2015.2421871.
Muhojoki, J., Hakala, T., Kukko, A., Kaartinen, H., Hyyppä, J., 2024. Comparing positioning accuracy of mobile laser scanning systems under a forest canopy. Sci. Rem. Sens. 9, 100121. https://doi.org/10.1016/j.srs.2024.100121.
Murphy, G.E., Acuna, M.A., Dumbrell, I., 2010. Tree value and log product yield determination in radiata pine (Pinus radiata) plantations in Australia: comparisons of terrestrial laser scanning with a forest inventory system and manual measurements. Can. J. For. Res. 40 (11), 2223–2233. https://doi.org/10.1139/X10-171.
Neudam, L., Annighöfer, P., Seidel, D., 2022. Exploring the potential of mobile laser scanning to quantify forest structural complexity. Front. Rem. Sens. 3, 861337. https://doi.org/10.3389/frsen.2022.861337.
Niemistö, P., 1992. Runkolukuun perustuvat harvennusmallit. Metsäntutkimuslaitoksen Tiedonantoja 432.
Niemistö, P., Kilpeläinen, H., Poutiainen, E., 2018. Effect of first thinning type and age on growth, stem quality and financial performance of a Scots pine stand in Finland. Silva Fenn. 52 (2), 7816. https://doi.org/10.14214/sf.7816, 21.
Noordermeer, L., Sørngård, E., Astrup, R., Næsset, E., Gobakken, T., 2021. Coupling a differential global navigation satellite system to a cut-to-length harvester operating system enables precise positioning of harvested trees. Int. J. For. Eng. 32 (2), 119–127. https://doi.org/10.1080/14942119.2021.1899686.
OSGeo. V.voronoi manual. GRASS GIS. n.d. Retrieved June 3, 2025. Available at: https://grass.osgeo.org/grass-stable/manuals/v.voronoi.html. (accessed on September 20, 2025).
Kohti automaattista puunkorjuun laadun mittaamista. English summary: towards automatic quality measurement in wood harvesting. In: Ovaskainen, H. (Ed.), 2019. Metsätehon Raportti 251. Metsäteho Oy. Available online at https://www.metsateho.fi/wp-content/uploads/Raportti_251_Kohti_automaattista_puunkorjuun_laadun_mittaamista.pdf. (Accessed 20 September 2025).
Ovaskainen, H., Riekki, K., 2022. Computation of Strip road networks based on harvester location data. Forests 13 (5), 782. https://doi.org/10.3390/f13050782.
Pohjala, J., Vahtila, M., Ovaskainen, H., Kankare, V., Hyyppä, J., Kärhä, K., 2024. Effect of prior tree marking on cutting productivity and harvesting quality. Croat. J. For. Eng. 45 (1), 25–42. https://doi.org/10.5552/crojfe.2024.2213.
Pohjala, J., Kankare, V., Hyyppä, J., Kärhä, K., 2025. Effects of a Mobile LiDAR-Based thinning density assistant (TDA) system on harvester operator performance. Eur. J. For. Res. https://doi.org/10.1007/s10342-025-01808-y.
Ponsse Plc. https://www.ponsse.com, 2022–. (Accessed 20 September 2025).
Purfürst, F.T., 2010. Learning curves of harvester operators. Croat. J. For. Eng. 31 (2), 89–97. https://doi.org/10.5552/crojfe.
Pyörälä, J., Kankare, V., Liang, X., Saarinen, N., Rikala, J., Kivinen, V.-P., Sipi, M., Holopainen, M., Hyyppa, J., Vastaranta, M., 2019. ' Assessing log geometry and wood quality in standing timber using terrestrial laser-scanning point clouds '. Forestry 92 (2), 177–187. https://doi.org/10.1093/forestry/cpy044.
R Core Team, 2025. R: a Language and Environment for Statistical Computing. R Foundation for Statistical Computing, Vienna, Austria. https://www.R-project.org/.

Saarinen, N., Kankare, V., Yrttimaa, T., Viljanen, N., Honkavaara, E., Holopainen, M., Hyyppä, J., Huuskonen, S., Hynynen, J., Vastaranta, M., 2020. Assessing the effects of thinning on stem growth allocation of individual Scots pine trees. For. Ecol. Manag. 474, 118344. https://doi.org/10.1016/j.foreco.2020.118344.

Sagar, A., Kärhä, K., Einola, K., Koivusalo, A., 2024. Assessing the potential of onboard LiDAR-based application to detect the quality of tree stems in cut-to-length (CTL) harvesting operations. Forests 15 (5), 818. https://doi.org/10.3390/f15050818.

Sagar, A., Kärhä, K., Järvelin, K., Ghabcheloo, R., 2025. Evaluation of simulation framework for detecting the quality of forest tree stems. Forests 16 (6), 1023. https://doi.org/10.3390/f16061023.

Salmivaara, A., Miettinen, M., Finér, L., Launiainen, S., Korpunen, H., Tuominen, S., Heikkonen, J., Nevalainen, P., Sirén, M., Ala-Ilomäki, J., Uusitalo, J., 2018. Wheel rut measurements by forest machine-mounted LiDAR sensors–accuracy and potential for operational applications? Int. J. For. Eng. 29 (1), 41–52. https://doi.org/10.1080/14942119.2018.1419677.

Sevgen, E., Abdikan, S., 2023. Classification of large-scale Mobile laser scanning data in urban area with LightGBM. Remote Sens. 15, 3787. https://doi.org/10.3390/rs15153787.

Siren, M., 1981. Puuston vaurioituminen harvennuspuun korjuussa. In: Summary: Stand Damage in Thinning Operations. Folia Forestalia, vol 474.

Siren, M., 1982. Puuston vaurioituminen harvennuspuun korjuussa kuormainprosessorilla. Folia For. 528.

Sirén, M., 1998. Hakkuukonetyö, sen korjuujälki ja puustovaurioiden ennustaminen [One-grip harvester operation, it's silvicultural result and possibilities to predict tree damage]. Metsäntutkimuslaitoksen tiedonantoja 694. Finnish Forest Research Institute. Available at https://urn.fi/URN:ISBN:951-40-1635-1. (Accessed 20 September 2025).

Sondell, J., 1974. Mätning av stickvägsareal. Skogsarbeten.

Strubergs, A., Zimelis, A., Kaleja, S., Ivanovs, J., Sisenis, L. i, Lazdins, A., 2024. Using cut-to-length (CTL) harvester production data in forest inventories. Croat. J. For. Eng. 45 (2), 277–292. https://doi.org/10.5552/crojfe.2024.2319.

Suunto, 2025. Suunto precision instruments – user guide. Suunto.

Tarmu, T., Laarmann, D., Kiviste, A., 2020. Mean height or dominant height – what to prefer for modelling the site index of Estonian forests? For. Stud. 72 (1), 121–138. https://doi.org/10.2478/fsmu-2020-0010, 2020.

ThinkGeo. GIS software company. https://thinkgeo.com/. (Accessed 20 September 2025).

Tørå, G.D., 1978. Sär pä traer ved tynningsdrift. Årsak,omfang og virking. En litteraturstudie. Tidsskr. Skogbruk 86 (3), 211–245.

Vastaranta, M., Saarinen, N., Kankare, V., Holopainen, M., Kaartinen, H., Hyyppä, J., Hyyppä, H., 2014. Multisource single-tree inventory in the prediction of tree quality variables and logging recoveries. Remote Sens. 6, 3475–3491. https://doi.org/10.3390/rs6043475.

Wang, Y., Lehtomäki, M., Liang, X., Pyörälä, J., Kukko, A., Jaakkola, A., Liu, J., Feng, Z., Chen, R., Hyyppä, J., 2019. Is field-measured tree height as reliable as believed – a comparison study of tree height estimates from field measurement, airborne laser scanning and terrestrial laser scanning in a boreal forest. ISPRS J. Photogrammetry Remote Sens. 147, 132–145. https://doi.org/10.1016/j.isprsjprs.2018.11.008.

White, J.C., Wulder, M.A., Varhola, A., Vastaranta, M., Coops, N.C., Cook, B.D., Pitt, D., Woods, M., 2013. A best practices guide for generating forest inventory attributes from airborne laser scanning data using an area-based approach. For. Chron. 722–723, 89.06. 10.5558/tfc2013-132. https://pubs.cif-ifc.org/doi/abs/10.5558/tfc2013-132.

Wielgosz, M., Puliti, S., Xiang, B., Schindler, K., Astrup, R., 2024. SegmentAnyTree: a sensor and platform agnostic deep learning model for tree segmentation using laser scanning data. Rem. Sens. Environ. 313, 114367. https://doi.org/10.1016/j.rse.2024.114367.

Xiang, B., Wielgosz, M., Kontogianni, T., Peters, T., Puliti, S., Astrup, R., Schindler, K., 2024. Automated forest inventory: analysis of high-density airborne LiDAR point clouds with 3D deep learning. Rem. Sens. Environ. 305, 114078. https://doi.org/10.1016/j.rse.2024.114078.

Xiang, B., Wielgosz, M., Puliti, S., Král, K., Krůček, M., Missarov, A., Astrup, R., 2025. ForestFormer3D: a unified framework for end-to-end segmentation of forest LiDAR 3D point clouds. arXiv. https://doi.org/10.48550/arXiv.2506.16991.

Yrttimaa, T., Liikonen, L., Erkkilä, A., Paakkari, J., Kotivuori, E., Vastaranta, M., 2025. Measuring Forest Inventory Attributes Using Faro Orbis Mobile Laser Scanner in Managed Boreal Forests. EGU General Assembly, Vienna, Austria. https://doi.org/10.5194/egusphere-egu25-18099. EGU25-18099.

Zhang, Hailong, Liu, Shirong, Yu, Jinyuan, Li, Jiwei, Shangguan, Zhouping, Deng, Lei, 2024. Thinning increases forest ecosystem carbon stocks. For. Ecol. Manag. 555, 121702. ISSN 0378-1127. https://doi.org/10.1016/j.foreco.2024.121702.